POLITECNICO DI TORINO

Master Degree in

Energy and Nuclear Engineering

Master of Science Thesis

OPTIMAL MANAGEMENT OF ELECTROCHEMICAL ACCUMULATORS AS A FUNCTION OF THE ENERGY BALANCE BETWEEN THE PREDICTED PRODUCTION FROM PHOTOVOLTAICS AND THE CONSUMPTION: A CASE STUDY

Tutors	**Candidate**
Prof. Filippo Spertino	Davide Fontana – S231187
Ing. Alessandro Ciocia	

A.Y. 2017-2018

I would like to thank my family and

everyone who encouraged me

during the writing of this Thesis

Contents

INTRODUCTION

Intermittent renewable energy sources such as wind and solar power are becoming more and more relevant in the world energy scenario. The diffusion of these clean sources is due to the cheap cost of their technology and to the growing subsidies in the renewable energy sector. Another advantage is the reduction of carbon dioxide emission and the mitigation of the so called "global warming". Beside these advantages, there are some problems concerning the diffusion in large scale of intermittent renewable energy sources such as the mismatch between power demand and supply. Another problem is the instability of the grid with possible disconnections and voltage reductions.

A way to face these matters consists in making use of storage systems which are able to store the excesses of energy deriving from wind or photovoltaic and use them when the energy demand from users is higher than the energy supply. Thanks to energy storage, it is possible to use the power from the sun at night or when the weather is cloudy with the reduction of electricity bought from the grid. The storage is also very important in isolated areas where it is used in combination with other power systems such as gas turbines or large diesel engines in order to provide power in case of fault or to cover the peak demand. Finally, energy storage is a powerful way to provide a regulation of the grid frequency reducing instabilities due to the penetration of renewables.

The most mature storage devices are lithium ion batteries due to their simplicity and their modularity with power ranging from some Kilowatts to some Megawatts. Another advantage of these electrochemical devices is the high energy density but also the fast power ramping with the fast reaching of the desired power.

The aim of this thesis is to improve the management of a storage system, composed of lithium ion battery modules, combined with a rooftop PV installation and located in the North West of Italy more precisely in Turin. The study is about a new Battery Management System (BMS) with a particular focus on the forecasted energy balance between PV production and household load. This allows to understand the amount of energy that can be drawn from the battery right now and the amount that should be left for the next day. The optimization of the battery management should guarantee the minimization of the maximum power absorbed from the grid without decreasing self-consumption. The Battery State of Charge (SOC) is maintained in a suitable range to avoid possible overcharging or undercharging conditions which could weaken the battery if no measure is adopted.

The PV production is then matched with the load profile of the household in order to understand when charging or discharging the battery in order to guarantee the satisfaction of the user demand. To do this task, a Matlab® model is applied to the system.

The thesis aims to demonstrate that the integration of storage and forecasted energy balance is able to minimize the contract power and besides it is a powerful method to achieve a more rational use of energy. The smart use of batteries becomes then a key factor to perform this task and to improve the grid state of health making it ready to welcome the continuous growth of intermittent renewable energy sources such as wind and solar.

CHAPTER 1: PHOTOVOLTAIC TECHNOLOGY

Solar energy is associated to solar radiation and represents the primary energy source on the earth. This source of energy can be used to produce both electricity and heat in a clean way reducing pollutant emissions *[1]*.

Photovoltaic plants, constituted by one or more photovoltaic modules, allow to directly convert solar radiation into electrical energy without the need of any fuel. Photovoltaic modules exploit the so called photovoltaic effect thanks to which some semiconductor materials, if accurately "doped", generate electricity if exposed to solar radiation with efficiencies that can reach 20%.

The electricity produced by a PV plant is related to several factors: incident solar radiation, tilt angle and orientation, the presence of shading and finally by the efficiency of auxiliary components such as inverters.

The main advantages of a PV plant are its modularity, the onsite production without any losses due to the transportation of energy, the absence of noise, the high reliability with a useful life of about 20 years and finally the possibility of recycling until 80% of the module weight.

Despite this, there are also some disadvantages such as the intermittent energy production, the low efficiency, the low energy density with the occupation of large surfaces and the high initial costs.

1.1 SOLAR RADIATION

The sun is made of 75% hydrogen, 23% of helium and 2% of other gases *[2]*. The inner layer of the sun has a temperature of 1.5 million of °C whereas the outer temperature is about 6000 °C. The energy produced by the sun is produced by the nuclear fusion reactions which convert hydrogen into helium.

When making calculations, the sun is approximated to an ideal radiation emitter (black body) with a surface temperature of about 5800 K. Outside the atmosphere, the spectral distribution of electromagnetic radiation varies from the ultraviolet to the infrared and has a maximum in the visible field for a value of wavelength equal to 0.5 μm. The corresponding power density that hits the unit area perpendicular to the earth radius is called *solar constant* G_{sc} and has a value of 1367 W/m^2.

$$G_{sc} = \frac{P_s}{4\pi r_{se}^2} = \frac{3.85*10^{26}}{4\pi*(1496*10^{11})^2} = 1367\,\frac{W}{m^2} \tag{1-1}$$

Where P_s is the power emitted by the Sun and r_{se} is the mean earth-sun distance.
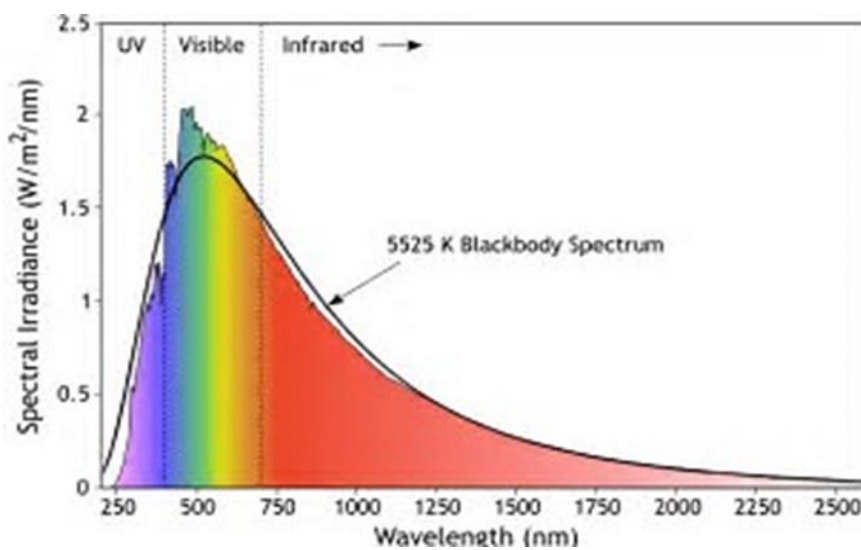
Figure 1.1: Spectral distribution of solar radiation

The power coming from a radiant source that hits the unit area is called *irradiance G[W/m^2]*. When solar radiation enters the atmosphere, part of the incident energy is lost due to *dispersion and reflection* or to *absorption [3] [4]*

Absorption is due to the presence in the atmosphere of ozone molecules in the UV band, of water vapour and carbon dioxide in the infrared range. Dispersion and reflection are due to the presence of molecules of nitrogen and oxygen but also to water drops and particulates. Dispersion phenomena strongly depend from the site and have maximum values in urban areas. Because of these phenomena, most of solar radiation that hits the earth has a wavelength between 0.29 µm and 2.5 µm.

Global solar radiation can be divided into:

- *Direct solar radiation G_b* constituted by the sun rays that hit the earth surface without angular deviation.
- *Diffuse solar radiation G_d* constituted by the part of the sun rays that are reflected by atmospheric gases varying the incidence angulation. Diffuse radiation is high when the weather is cloudy but depends also on altitude, latitude and location.
- *Albedo G_a* that is made of the part of radiation that, after being reflected by the earth surface, can reach a receiver.

The total solar radiation that hits a receiver on the earth surface can be written as the sum of these three contributes.

$$G = G_b + G_d + G_a \qquad\qquad\qquad (1\text{-}2)$$
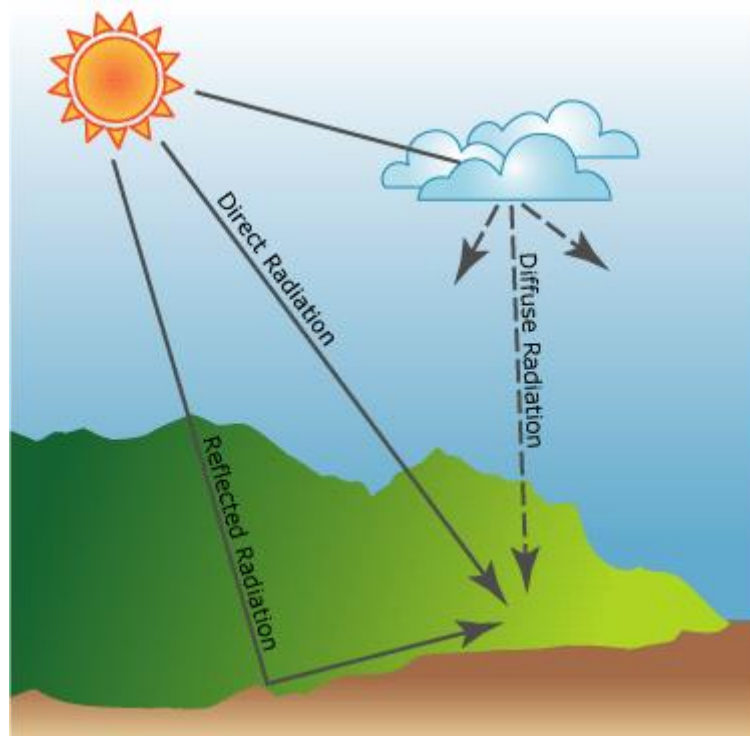
Figure 1.2: Behaviour of solar radiation in the atmosphere

Finally, the irradiance integrated on a time interval is defined as *irradiation H,* whose unit of measure is kWh/m^2.

$$H = \int_{t1}^{t2} G(t)dt \tag{1-3}$$

Where G is the total solar radiation and t_1 and t_2 are the boundary of the time interval considered. For the PV system design it is necessary to know the daily, monthly and annual irradiation.

1.2 AIR MASS

The influence of the terrestrial atmosphere on solar radiation which hits the ground at a certain instant is taken into account through a parameter called *Air Mass (AM)*. This parameter is equal to the ratio of the mass of atmosphere crossed by the direct solar radiation and the one that this radiation would have crossed if the Sun had been to Zenith. On a sunny summer day, at sea level, the radiation coming from the Sun at Zenith is equal to a unit Air Mass (AM=1). In other weather conditions, air mass is approximately equal to:

$$AM = \frac{1}{cos\theta_z} \ or \ AM = \frac{1}{P_0 sin\theta_z} \tag{1-4}$$

Where:

$-P_0$ is the reference pressure equal to $1.013 \cdot 10^5$

$-\theta_z$ is the angle between the line Earth-Sun and the Zenith direction perpendicular to the horizontal plane.
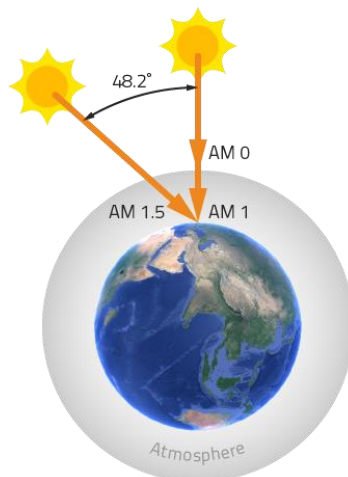

Figure 1.3: Correlation between AM and Zenith angle

1.3 MEASUREMENT OF SOLAR RADIATION

Solar radiation is measured thanks to *Solarimeter* and *Pyranometer*. The pyranometer is an instrument used to measure the global solar radiation which hits a surface. The working principle is based on the temperature difference between a clear surface and a dark surface. The dark surface absorbs the most of solar radiation whereas the clear one tends to reflect absorbing just a little of the radiation. The temperature difference is measured thanks to a thermopile. The potential difference generated inside the thermopile allows to measure the value of the incident solar radiation.
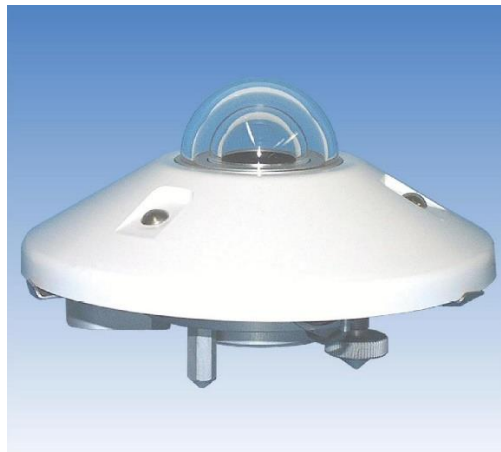
Figure 1.4: Pyranometer

Solarimeter, instead, is based on the photovoltaic effect with the same behaviour of a PV cell: it generates an electrical signal according to the incident radiation measuring especially the visible light with a response that depends on the cell temperature. Values measured by a solarimeter which uses the photovoltaic effect have to be corrected taking into account the temperature.

Figure 1.5: Solarimeter

1.4 WORKING PRINCIPLE OF THE SOLAR CELL

In order to fully understand the photovoltaic conversion of energy it is necessary to explain two important concepts that is *the energy band* and *the photovoltaic effect*.

1.4.1 ENERGY BAND

The energy bands are the totality of energy levels that an electron can assume. The energy bands can assume three different states:

- *Valence band* made of electrons involved in the bonds within two atoms

- *Conduction band* made of electrons that can leave their corresponding atoms and move across the crystalline reticule giving rise to an electric conduction

- *Valence jump* that is the energy needed to take an electron from the valence band to the conduction band

The valence jump or *Energy Gap E_g* is an important quantity that varies with the considered materials: it is very high for insulating material, it is limited for semiconductors and it is nearly null for conductors.

E_g = 1.1 eV (Si) ; E_g = 0.67 eV (Ge) ; E_g = 1.41 eV (GaAs)

(a) Insulator   (b) Semiconductor   (c) Conductor
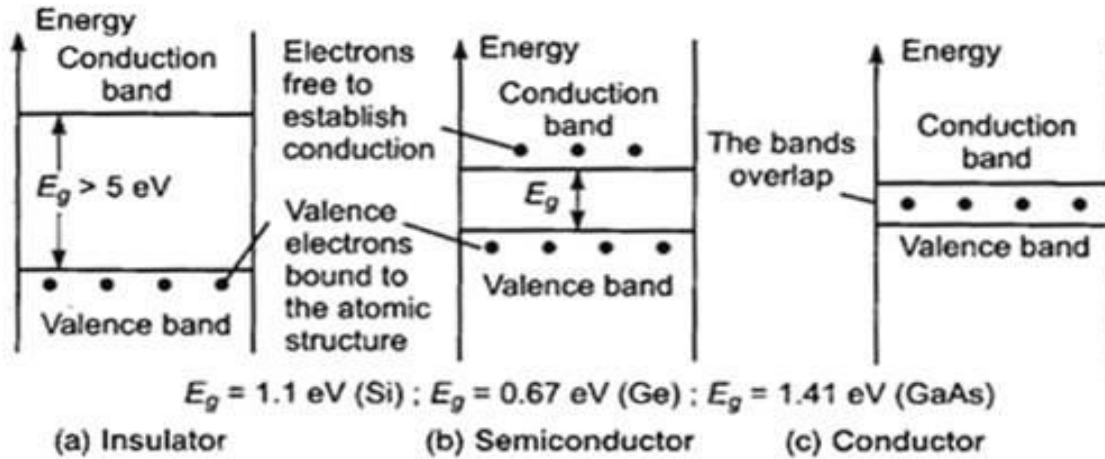
Figure 1.6: Energy gap for different kinds of materials.

1.4.2 PHOTOVOLTAIC EFFECT

The photovoltaic effect consists in the emission of electrons from a surface once that this surface is hit by an electromagnetic radiation made of photons which have a certain wavelength. The photovoltaic effect occurs only if the photon has sufficient energy to break the bonds that connect the electrons to the atoms. This minimum energy is determined by the formula:

$$E_{ph} = h * f = h * \frac{c}{\lambda} \geq E_g \tag{1-5}$$

Where E_{ph} is the photon energy [J], h is the Planck constant ($6.625*10^{34} J * s$), f is the frequency [Hz], c the speed of light (300000 km/s), λ the wavelength (m) and finally E_g [J] is the energy gap.

Once that the electron moves from the valence band to the conduction band it generates a hole in the valence band.

1.4.3 LAYOUT AND WORKING MECHANISM OF A SOLAR CELL

The most widespread solar cells in commerce are of three types: monocrystalline silicon, polycrystalline silicon and thin film cells. The solar cells are generally square shaped but they can be also pseudo square shaped or rectangular shaped.

In order to exploit the electricity generated by the solar cell, it is necessary to create a motion of electrons and holes by providing a suitable electrical field. This field is created by adjusting a layer of positively charged fixed atoms in one side of the semiconductor cell and a layer of negatively charged atoms in the other.

This procedure is achieved thanks to a "doping" treatment that is by inserting some impurities made of atoms belonging to the third or fourth group of the periodic table. By doing this, a motion of electrons from the n junction (negatively charged) to the p junction (positively charged) and vice versa is created. If there is a connection between the p-n junction and a conductor, a flux of electron starts moving in the external circuit passing from the n layer to the p layer. Until the cell is exposed to the sun light, the electricity will keep on flowing under the form of direct current.

It is important that the n layer, the one exposed to sunlight, can guarantee the maximum absorption of incident photons in proximity of the junction: so the width of the n layer has to be about 0.5 mm and the width of the whole cell must not exceed 250mm. In the solar cell, hit by the sunlight, there will be the production of a current I_{ph} proportional to the irradiance G.

$$I_{ph}[A] \propto G \left[\frac{W}{m^2}\right] \tag{1-6}$$

It is important to underline the just a part of solar radiation that hits the cell is converted into electrical energy and so many losses factors have to be considered.

The most important ones are:

- Reflection of photons on the cell surface (~10%): not all the photons penetrate inside the cells, some are reflected by the surface and others hit the metallic frame. To avoid these losses antireflection treatments are adopted.

- Surplus or deficit in the energy content of photons (~50%): if the photons have not sufficient energy they are not able to break the bonds that involve the electrons otherwise if they are too energetic they dissipate their surplus of energy into heat.

- Recombination (~2%): the electrons could recombine with charges of different sign without being sent to the external circuit.

- Parasitic resistances (~20%): These losses are related to the Aluminium-Silicon interface where the resistances located there provoke a dissipation which reduces the power transferred to the load.

Because of these losses, the efficiencies of monocrystalline silicon photovoltaic cell is generally between 13% and 20% whereas some special laboratory applications have reached an efficiency of 30%.
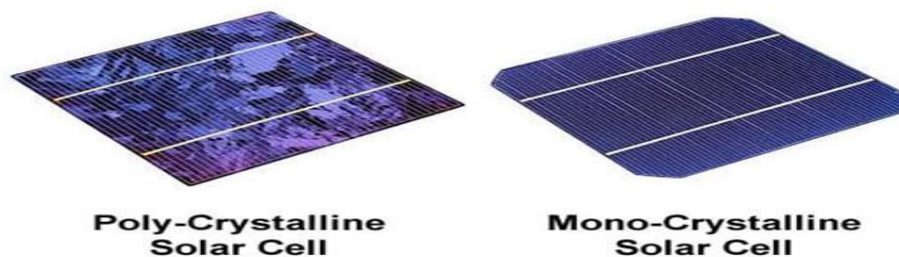
Figure 1.7: monocrystalline and polycrystalline solar cell

1.4.4 THE EQUIVALENT CIRCUIT OF A PHOTOVOLTAIC CELL

The equivalent circuit of a solar cell is made of an ideal current generator, proportional to the irradiance, a real diode and two dissipative elements, that is a parallel resistor R_{sh} and a series resistor R_s to the circuit.
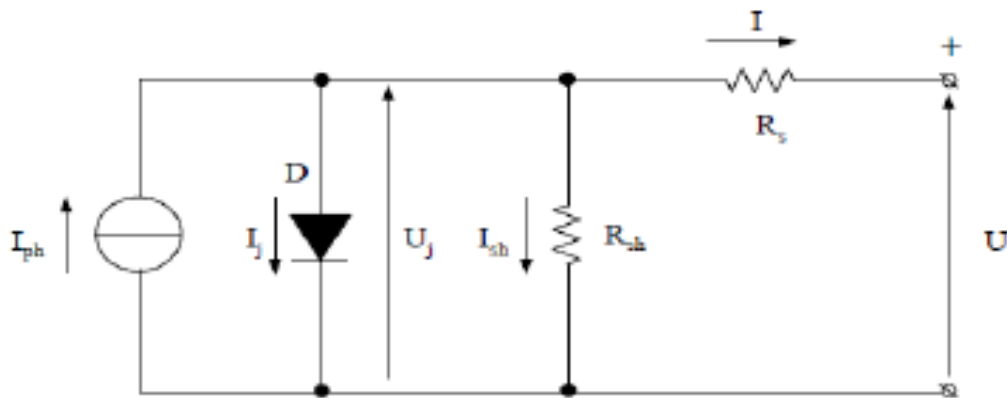
Figure 1.8: The equivalent circuit of a solar cell

The R_{sh} corresponds to the surface current dispersion between the plate and the grate, R_s accounts for the volume resistance of the semiconductor, the contact resistances and the ones of the electrodes.

Every electron contribute to the formation of the photovoltaic current according to the equation:

$$I_{ph} = qNS \tag{1-7}$$

Where q $[1.6*10^{-19}eV]$ is the electron charge, N $[1/cm^2 * s]$ is the number of photons and S $[cm^2]$ is the area of the semiconductor which is exposed to sunlight.

The diode D makes the charge flow in a unique direction along the p-n junction. The current that crosses the diode can be expressed as:

$$I_j = I_0 * \left(e^{\frac{qU_j}{mKT}} - 1 \right) \tag{1-8}$$

Where K [$1.38*10^{-23}$ J/K] is the Boltzmann constant, $I_0 [A]$ the inverse saturation current of the diode, U_j [V] the voltage at the ends of the diode, m is the emission coefficient of the junction.

The current delivered to the load $I[A]$ can be expressed as:

$$I = I_{ph} - I_0 * \left(e^{\frac{qU_j}{mKT}} - 1 \right) - \frac{U_j}{R_{sh}} \tag{1-9}$$

Whereas the voltage on the load has the following expression:

$$U = U_j - R_s I \tag{1-10}$$

By considering the previous equations (1-9) and taking into account that $R_s \ll R_{sh}$ the voltage U can be written as:

$$U = \frac{mKT}{q} \ln \left(\frac{I_{ph}+I_0-I}{I_0} \right) - R_s I \tag{1-11}$$

This last equation describes the behaviour of the voltage transferred to the load when varying the current generated by the solar cell. The working characteristics is described by a voltage-current curve.
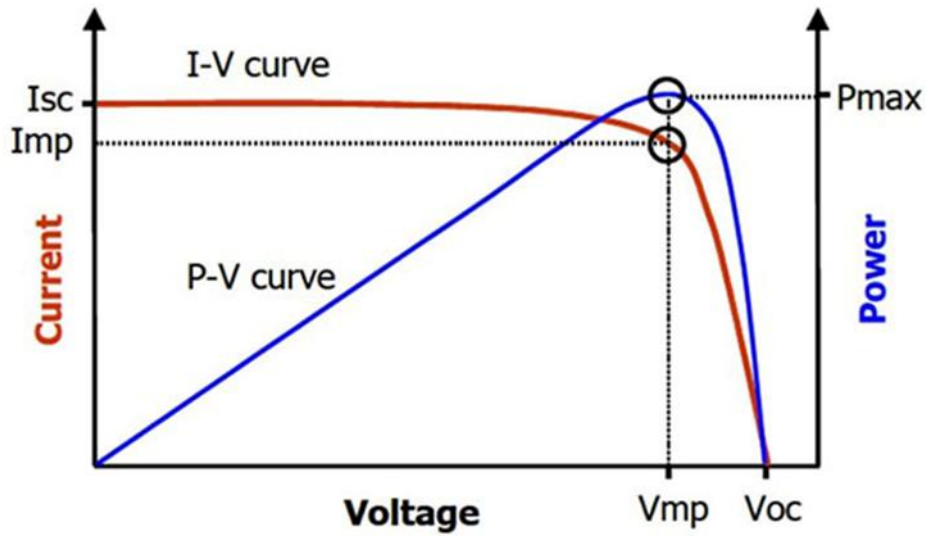
Figure 1.9: I-V curve and P-V curve of a solar cell.

By analysing this curve it is possible to identify the *maximum power point* of coordinates (V_{mp}, I_{mp}) which is between two significant points: the short circuit in which the current is maximum ($I = I_{sc}$) and the voltage is zero and the open circuit in which the voltage is at its peak ($V = V_{oc}$) and the current is null. Another important parameter of the solar cell is the *fill factor* (K_f) defined as:

$$K_f = \frac{V_{mp}I_{mp}}{V_{oc}I_{sc}} \tag{1-12}$$

This last parameter represents globally the influence of the diode and of the resistors R_{sh} and R_s on the characteristics of the cell. Typical values of the fill factor for crystalline silicon PV cells are between 0.7 and 0.8.

1.4.5 DEPENDENCE ON IRRADIANCE AND TEMPERATURE

The characteristic I(U) of a solar cell, at constant temperature T_{PV}, changes if a variation in the irradiance G occurs. If G decreases the short circuit current decreases proportionally whereas the open circuit voltage decreases logarithmically. U_{oc} remains nearly constant as the irradiance decreases but drops down sharply if the irradiance goes below 50 W/m^2.

As regards silicon solar cell, the I(U) characteristics changes very rapidly as G varies with a time range between 10μs and 20 μs.
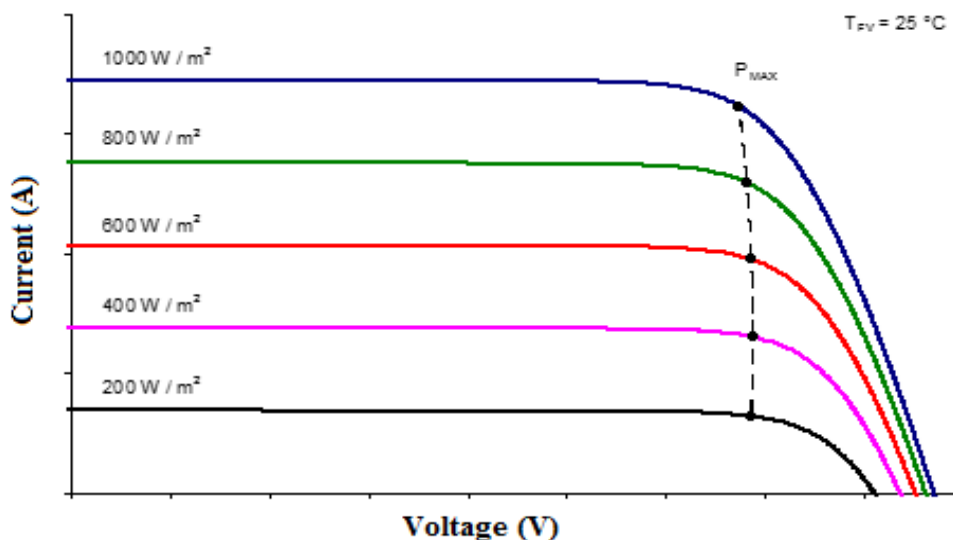
Figure 1.10: I(U) characteristic with variation in the irradiance

There is also a dependence of I(U) characteristics from the temperature T_{PV}.

At constant irradiance, the temperature increase provokes a little increase in the photovoltaic current and thus of I_{sc} due to the reduction of the bandgap.

Another effect is the increase of the diode current I_j which determines a reduction of U_{oc} with an incremental ratio dU_{oc}/dT_{PV} equal to -2.2 mV/°C for each cell. The thermal gradient of the

maximum power due to these variations is nearly constant. In real applications, the short

circuit current I_{sc} is supposed to depend only on the irradiance G whereas the open circuit

voltage U_{oc} only on the temperature T_{PV}.

G = 1000 W / m²

$T_{PV} = 0°C$

$T_{PV} = 20°C$

$T_{PV} = 40°C$

$T_{PV} = 60°C$
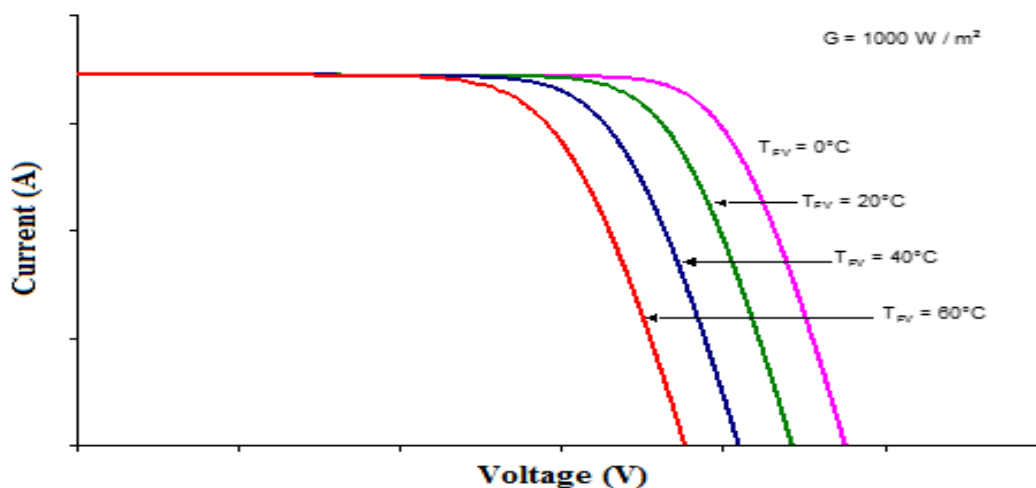
Figure 1.11: I(U) characteristic with variation in the temperature

1.4.6 SERIES AND PARALLEL CONNECTION OF SOLAR CELLS

A single PV cell made of silicon, with optimal irradiance and load conditions, generates a

voltage of about 0.4÷0.6V, independently from the lighted surface. The current, instead,

depends on surface with typical values of current densities equal to 0.2÷0.3 mA/mm^2.

Loads currently used require voltages and currents much higher with respect to the ones

provided by the single cells. In order to get the required power, it is necessary to connect more

solar cells in series or in parallel thus originating the *photovoltaic module*. During the normal

operation, the characteristics of the PV module show some variations due essentially to two

reasons: the natural variation of parameters due to defects in manufacturing and the various working conditions that occur (ex. Some cells belonging to the module are shaded). These variations provoke a reduction of the performances of the PV module and are referred to the so called *mismatching*. The mismatch can provoke several problems according to the connection of the cells.

Series connection

If N_s identical cells are series connected and one of them has a characteristic which differ from the others, for example because of partial shading, the resulting characteristics is given by the sum, for a given current, of the voltage of the not shaded $N_s - 1$ cells and of the voltage of the shaded cell.
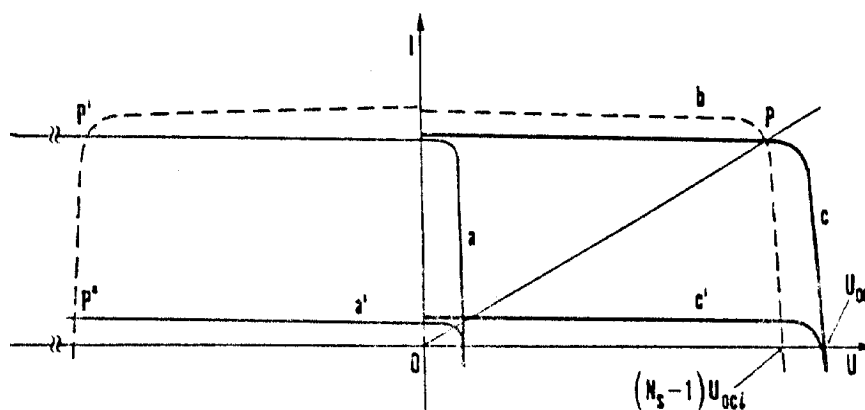

Figure 1.12: I-U characteristic of series connected cells in case of mismatch

- Curve a: different from the others because of manufacturing defects.

- Curve a': different from the others because of shading.

- Curve c: resulting characteristic (for the curve a) , for a given current, of the voltage of the $N_s - 1$ equal cells plus the voltage of the cell with a manufacturing defect.

- Curve c: resulting characteristic (for the curve a') , for a given current, of the voltage of the $N_s - 1$ equal cells plus the voltage of the shaded cell.

- Curve b: resulting from the sum of the characteristics of $N_s - 1$ normally operating cells.

The maximum generated power is anyway always lower than the sum of the maximum powers of the series connected cells. The resulting curve has an open circuit voltage U_{oc} equal to the sum of the $U_{oc,i}$ of the single cells and a short circuit current I_{sc} equal to the one of the cell which generates the lowest current.

If the cell is completely shaded, it stops generating current and starts opposing to the current flux generated by the other cells and with its own resistance generates a voltage opposed to the ones of the other cells. The shaded cells becomes then a load and it will dissipate heat creating a hot spot (point P' of Figure 1.12). If the voltage $(N_s - 1)U$ exceeds the maximum break down voltage U_b, the immediate destruction of the cell occurs.

A diode D_P parallel connected to the shaded cells avoids that this cells operates as a load with an inverse voltage.
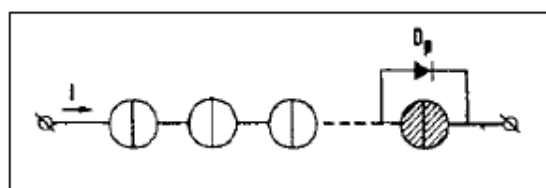

Figure 1.13: Protection Diode parallel connected to the solar cell

The diode D_P has the task not to limit the short circuit current of the string to the value of the short circuit current of the cell with the worst characteristic (a') but instead the diode should make it equal to the one of the remaining series connected cells with the best characteristics.

Parallel Connection

As for the series connection, if N_P are parallel connected and one cell show a different characteristic from the other cells (for example because of shading), the resulting characteristics is given by the sum, for a given voltage, of the currents of the $N_P - 1$ not shaded cells and of the one of the shaded cell. The resulting characteristic has a short circuit current I_{SC} equal to the sum of $I_{SC,i}$ of the single cells and an open circuit voltage U_{OC} very close to the one of the shaded cell. If one cell is shaded, the parallel of the cells behaves towards the load as the parallel of $N_P - 1$ lighted cells. The worst condition for the shaded cell is with a null external load because in this condition the shaded cell is obliged to absorb the current of the $N_P - 1$ lighted cells.

A diode D_S series connected to the cell in parallel could avoid that the shaded cells works as a load with an inverse current.
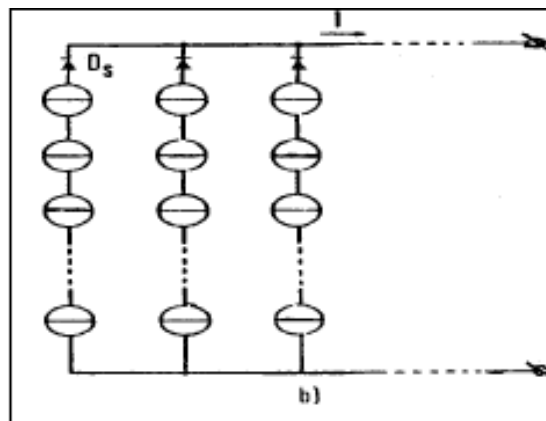
Figure 1.14: Protection Diode series connected to the strings in parallel

This protection is anyway not acceptable for the parallel of single cells since the voltage drop across the diode is of the same order of the generated voltage but it is applicable in case of strings composed of several cells in series.

1.5 PHOTOVOLTAIC MODULE DESCRIPTION

The manufacturing process of crystalline silicon photovoltaic modules consists chronologically in the following steps: electrical connection, encapsulation, insertion of the frame, insertion of the junction box and finally monitoring tests. *[5] [6] [7] [8] [9]*
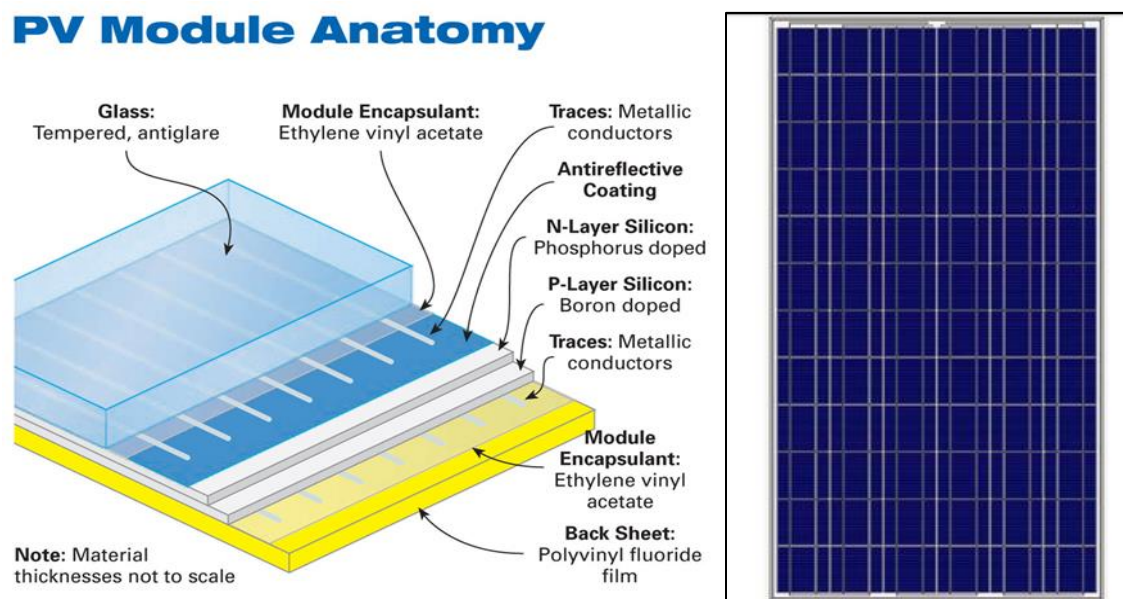
Figure 1.15: PV Module Anatomy

The *electrical connection* consists in a particular welding of the single solar cells in order to get the desired values of voltage and current.

The *encapsulation*, instead, consists in fixing the cells to a glass slab with a transparent adhesive film generally made of EVA ("ethylene vinyl acetate") and then inserting in the rear part of the cell another EVA film and a synthetic cladding made of Tedlar.

The encapsulation has to perform some important tasks: protect the cells, be transparent to solar radiation, stable to UV rays, with self-cleaning and temperature control capabilities.

The *frame* is generally made of anodized aluminium and has the task of giving the module a higher robustness and allow the fixation to support structures.

The *junction box,* made of plastic material and mounted on the back side, contains the by-pass diodes and, in case of fault of the modules, it has to isolate the module from the whole plant. At the end of the manufacturing process, the cells are visually checked to find the damaged ones. By using an "artificial sun", the parameters I_{sc}, U_{oc}, P_{max} are determined.

This last phase is very important because it allows to give the customer modules with similar characteristics to the wished ones in order to reduce the losses due to *mismatch.*

Instead, as regards amorphous silicon, new manufacturing processes and techniques are getting more and more important.

For this kind of modules, the most diffuse technique consists in depositing directly the amorphous silicon on the glass slab which will constitute the transparent protection avoiding the use of sealant.

1.5.1 PHOTOVOLTAIC MODULE PERFORMANCE

The solar power P_S which hits the PV module in standard conditions, that is when G=1000W/m^2, T=25°C and the air mass is equal to 1.5, can be calculated as:

$$P_S = G * A \qquad (1\text{-}13)$$

Where A [m^2] is the whole area (including the frame) of the irradiated PV panel.

If P_m is the peak power [W_p] then the global efficiency of the PV module is expressed as:

$$\eta_m = \frac{P_m}{P_S} \qquad (1\text{-}14)$$

But the global efficiency can be also expressed as the product of three partial efficiencies:

$$\eta_m = \eta_P \eta_{Ec} \eta_{Im} \qquad (1\text{-}15)$$

η_P is the *filling efficiency* which takes into account only the part of the module constituted by solar cells and not by the frame, η_{Ec} is the *encapsulation efficiency*, whereas *non uniform irradiance efficiency* η_{Im} considers the fact that not all the cells of the PV module can be hit by the same irradiance.

1.6 PHOTOVOLTAIC PLANTS

In order to obtain the desired power it is necessary to connect the single PV modules. In the photovoltaic terminology, it is possible to state that more cells connected between them create a *module*.

The electrical and mechanical connection of these modules create a *panel*.

The series connection of these panels gives rise to an *array* and finally the parallel connection of the arrays constitute the *photovoltaic generator*.
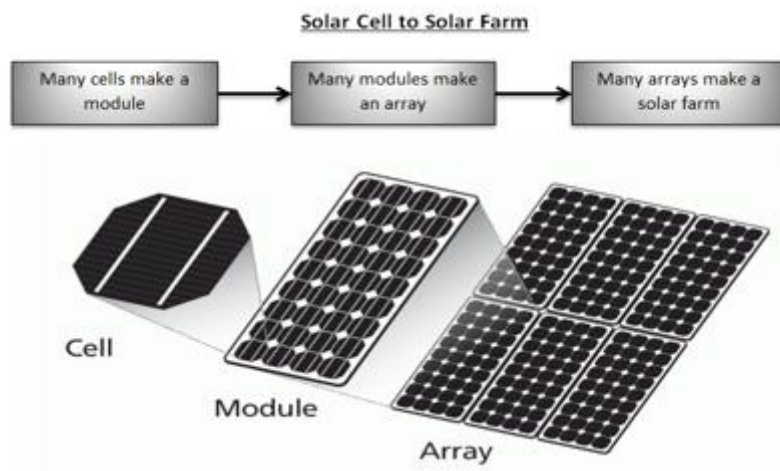
Figure 1.16: Photovoltaic terminology

Because of the mismatch between the arrays due to shading, non-uniform irradiation and occasional faults, it is important to insert some *by pass diodes* D_P in order to avoid the circulation of an inverse current between the arrays.

Moreover, to avoid the asymmetries in the parallel connection of the arrays, a *blocking diode* D_S is inserted in series to them.

Finally, it is important to perform an optimal connection between the modules.

They can be connected in series or in parallel. With a series connection, the exiting voltage is equal to the sum of the exiting voltage of the single cells whereas the exiting current is equal to the one of the single cell.

With a parallel connection, the output current is the sum of the one of the single elements whereas the output voltage does not vary.
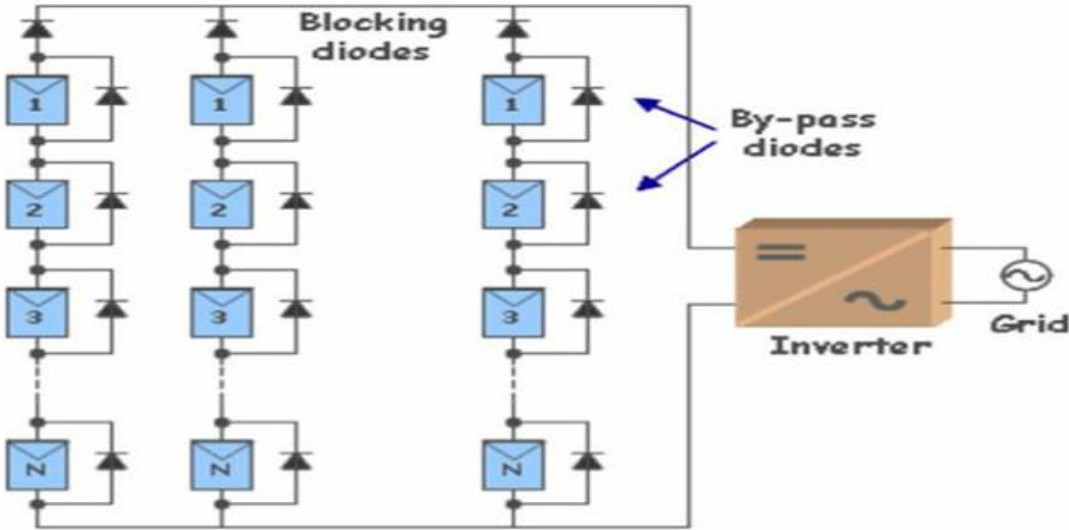
Figure 1.17: Blocking diodes and By-pass diodes in a PV solar field.

1.6.1 STAND ALONE AND GRID CONNECTED PV PLANTS

PV plants can be classified into two main categories: Stand-alone PV plant and grid connected PV plant.

STAND ALONE PV PLANTS

These kind of plants are not connected to the electrical grid and are composed by PV panels and generally by a storage system that guarantees the continuous production of electrical energy even in case of weak illumination or at night time. These plants are technically and economically advantageous when the electrical grid is absent or difficult to reach substituting sometimes the emergency diesel generators.

The stand-alone PV plant is often oversized in order to allow, during the day time, both the load feeding and the recharge of storage batteries.

GRID CONNECTED PV PLANTS

Grid connected PV plant absorb electrical energy from the grid in the periods in which the PV plant is not able to provide enough energy to satisfy the customer load. Vice versa, if the PV production is higher than the load, the excess of energy is injected into the grid.

These systems need a storage system only when the goal is to maximize the self-consumption of energy.

1.6.1 EXPOSURE OF PV MODULES

In order to correctly size a PV plant, it is important to know some parameters that describe the trajectory of the Sun in the different periods of the year in order to determine the solar power which hits a surface with a certain orientation and inclination and localized in a well-defined place.

These parameters are:

- The *latitude* which is the angle between the line which connects the place with the Earth centre and the equatorial plane.

- *Solar azimuth* γ_s which is the angle created by the projection on the horizontal plane of the line which connects the Sun and the Earth in the reference place with the south semi axis.

- *Solar height* α_s which is the angle between the line joining the Sun and the Earth in the reference place with the horizontal plane.

- *Surface azimuth* of plane γ which is the angle between the projections on the horizontal plane of the perpendicular to the surface in question with the South semi axis. Its optimal value is 0°, that is the surface is south oriented, otherwise with a West orientation it is possible to avoid the risk of mist in the afternoon.

- *Tilt angle β* which is the angle between the surface and the horizontal plane.
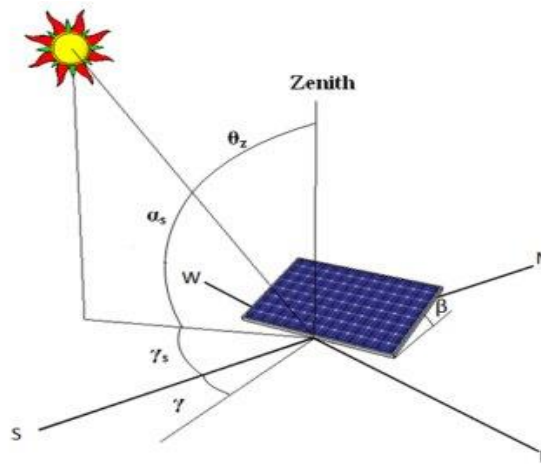
Figure 1.18: Graphical visualization of PV angles

Thanks to the regulation of the tilt angle β, it is possible to maximize the solar power which hits the PV module. The optimal β angle is higher in winter months with respect to summer months because of the low value of the Sun height in winter.

So the optimal tilt angle has a value which is between 0° and 90° allowing good performances in the winter months and reducing them a little in summer months when usually there is an over production of electrical energy.

Finally, the minimum distance between the parallel arrays of PV module has to avoid the phenomenon of *shading*.

The calculation is done by considering the winter solstice that is when the solar height is minimum. The formula is the following:

$$d_{min} = m\frac{sin\beta}{tan\alpha} \tag{1-16}$$

Where *m* is the length of the module.

1.6.2 THE INVERTER

The inverter is a component of the PV plant that converts the direct current into alternate current by checking the quality of the power output for the grid injection even thanks to a L-C filter.

The inverter is characterized by a high efficiency even at low loads. The expression of the inverter efficiency can be written as:

$$\eta_{inv} = \frac{P_{AC}}{P_{DC}} = \frac{V_{AC}I_{AC}cos\varphi}{V_{DC}I_{DC}} \qquad (1\text{-}17)$$

Where $cos\varphi$ is the power factor that is the lag between voltage and current, V_{AC} and I_{AC} are the voltage and the current in the AC side whereas V_{DC} and I_{DC} are the voltage and the current in the DC side.

The *inverters with transistor* are used as static switches and are controlled by opening and closing signals that, in the roughest case, give a square wave in output.

To avoid the generation of a square wave in output, the Pulse Width Modulation (PWM) is adopted. This technique is suitable to get a regulation both on the frequency and on the root mean square of the output waveform.

The main components of a single phase PWM inverter are:

- The *condenser C_{rip}* which reduces the variations on the instantaneous power
- The *LC filter* in order to get a waveform very similar to the sinusoidal one
- The *transformer* to get the desired voltage that is the one supplied to the load
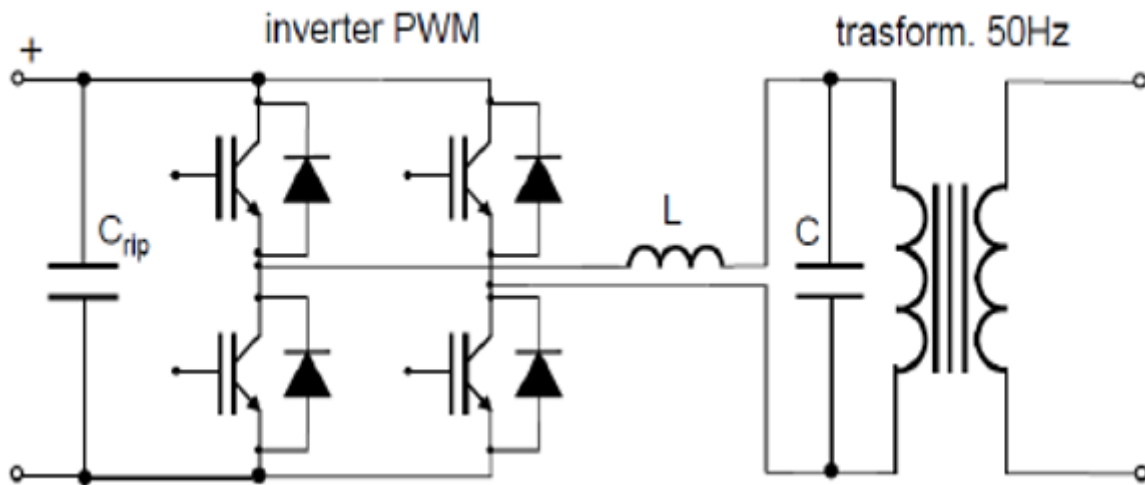
Figure 1.19: Single phase PWM inverter coupled with a low frequency transformer at 50 Hz

In order to optimize the energy production from the PV plant, the generator has to be well synchronized with the load in order to work at the maximum power all the time.

To do this, a component called *Maximum power point tracker (MPPT)* is used. The MPPT finds at every instant the voltage and the current which maximize the power output.

The maximum power point lays at the tangency between the IV curve of the PV generator and the hyperbole of equation IV=const.

By varying a little the load, the MPPT checks if the product of I and V is higher or lower than the previous one; if it is higher the variations of the load go on in the same direction otherwise they change in the other direction.

Maximum Power Point trackers are penalized by sudden variations in the solar irradiance or by shading phenomena, concentrated on a large part of the PV module, which can determine a large reduction of the maximum power voltage.

The inverters belonging to stand alone PV systems have to supply a voltage as constant as possible whereas the ones belonging to grid connected PV systems have to supply a voltage as similar as possible to the one of the electrical grid.

The inverter is optimally sized when the ratio between the active power injected into the grid and the nominal power of the PV generator is between 0.8 and 0.9.

The inverter is also provided with an automatic limitation of the output power to face the situations in which the generated power is higher than the forecasted one.
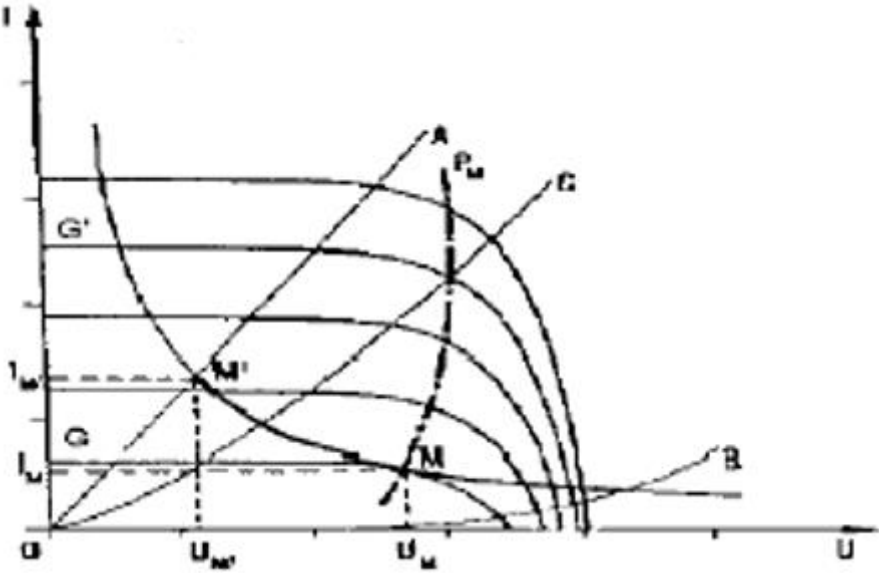
Figure 1.20: MPPT working principle for a PV generator

1.6.3 ESTIMATION OF ENERGY PRODUCTION

An important issue when dealing with the design of a PV plant is the estimation of energy production [10] [11] [12].

The formula used to evaluate the annual energy production is the following:

$$E_{AC} = G_{STC} S_{PV} \eta_{STC} h_{eq} PR \qquad (1\text{-}18)$$

Where $G_{STC} [W/m^2]$ is the irradiance measured in Standard Test Conditions, $S_{PV} [m^2]$ is the total surface of the PV generator, η_{STC} is the nominal efficiency of modules and finally $h_{eq} [\frac{h}{year}]$ represents the equivalent solar hours per year which can be calculated as the ratio between the *global irradiation* on the tilted plane and the STC irradiance.

PR is the Performance Ratio that is a parameter useful to match PV plants. The PR accounts for:

- Intrinsic mismatch of I-V curves of modules
- Dirt and reflection of frontal glass
- Diodes, fuses and switches
- Temperature higher or lower than 25°C
- Shading effect
- DC/AC conversion

CHAPTER 2: ENERGY STORAGE - APPLICATIONS

It is not easy to store electrical energy since usually it has to be produced when needed by the customer. The increasing diffusion of intermittent renewable energy sources made storage a necessary issue. Energy storage is able to give a great contribute for the stabilisation of grid providing frequency and voltage regulation and increasing then grid efficiency and reliability. Storage systems store electrical energy and convert it into another form of energy such as electrochemical, mechanical, electrical or thermal energy. The most general classification of storage systems is then based on *energy conversion modality*.
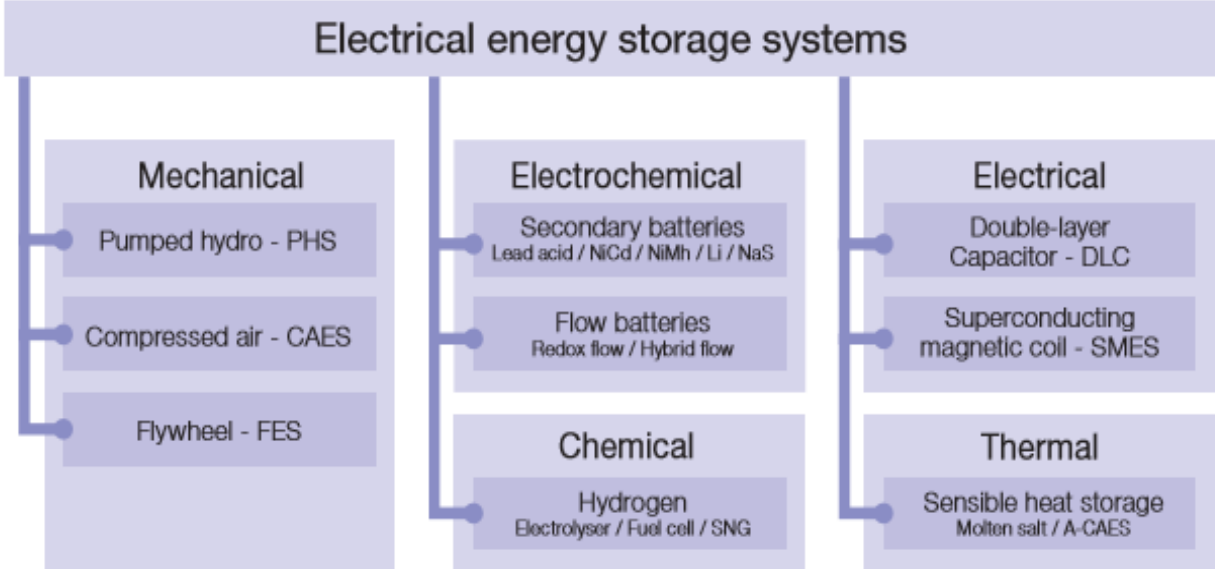

Figure 2.1: Storage system technologies

The most ancient and the most well-known form of energy storage is represented by Pumped Hydro Storage (PHS) whereas the most promising ones are SMES, DLC, Flywheels and batteries.

Pumped Hydro Storage (PHS)

Figure 2.2: PHS power plant

Pumped Hydro Storage systems use two water reservoirs at two different elevations. During off peak hours, water is pumped from the lower reservoir to the upper one charging the storage. When needed, water flows from the upper reservoir to the lower one powering a turbine coupled with an electrical generator (discharging phase).

Nowadays reversible pump-turbines with motor-generators are available. Discharge times range between several hours to a few days whereas the efficiency is between 70% and 85%. The main advantage of this technology is the long lifetime and the unlimited cycle stability of installation. Main drawbacks are the dependence on topographical conditions and the large land use.

Superconducting Magnetic Coil (SMES)

SMES are characterized by the presence of superconducting coil of high inductance L_{coil} kept at cryogenic temperature[13]. SMES stores energy in the magnetic field generated by the DC current I_{coil}. Power conversion is performed in two ways; the first one uses a current source converter (CSC) to interface the AC system and charge/discharge the coil, the other one makes

use of a voltage source converter (VSC) and a DC/DC chopper with a control of the voltage across the SMES coil V_{coil}.
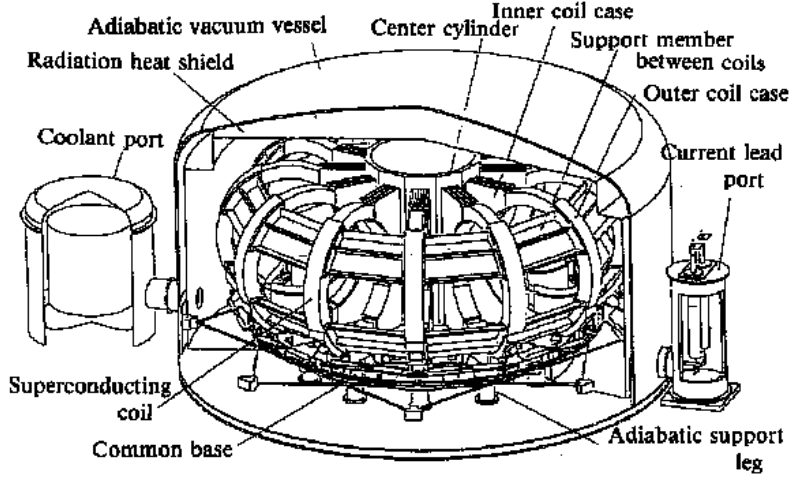
Figure 2.3: Schematic of a Superconducting magnet

Double Layer Capacitor (DLC)
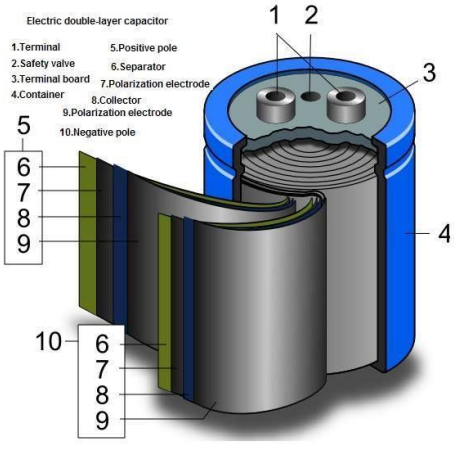
Figure 2.4:DLC storage system

SC rating can reach up to 5000 Farads whereas its highest energy density is about 30 Wh/kg *[13]*. Due to the close proximity of the electrodes, SCs can withstand a low voltage typically 2

or 3 Volt. SCs store energy by separating positive and negative charges and have an exceptional power density since the charges are physically stored on the electrodes.

On the other hand, energy density is low because the electrons are not bounded by chemical reactions. The combination of SC and battery energy storage can be found in electric vehicle and wind energy applications.

Flywheel Energy Storage (FES)

Flywheels store energy in the form of rotational kinetic energy by accelerating a rotor to a very high speed. Adding energy to the system makes flywheel speed increase. As regard the speed, it can vary from 20000 rpm to 50000 rpm. FES is characterized by a high energy density (100-130 Wh/kg), long lifetime, large maximum power outputs and a high energy efficiency (typically 90 %). Flywheels can also be used as frequency and power quality regulators in grid with large penetration of intermittent renewable sources.
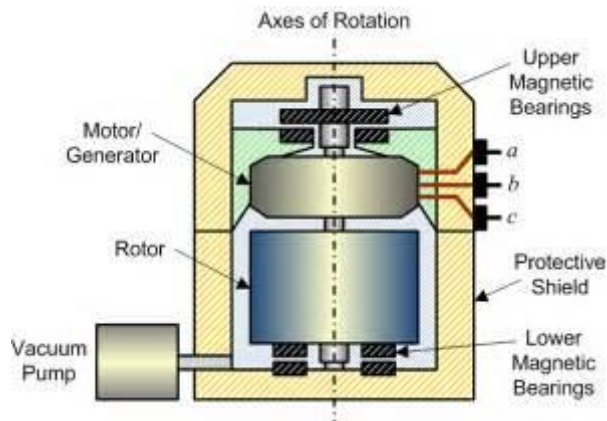
Figure 2.5: Schematic of a Flywheel Energy Storage

2.1 BATTERY STORAGE

Battery are made of a combination of a series connected or parallel connected electrochemical storage systems *[14]*. Batteries contain two half cells, each one made of a metal electrode called *cathode* and *anode,* submerged in an electrolytic solution containing ions of the same metal. Globally, inside the battery, a redox reaction occurs in which a chemical species (reducing agent) loses electrons getting oxidized and a second chemical species gets the electrons lost by the reducing agent and gets reduced.

It is then possible to consider the global reaction as divided into two sub reactions, physically separated and associated each one to a specific electrode. During the discharge phase, the electrons migrate from anode to cathode thanks to the external electrical conductor.
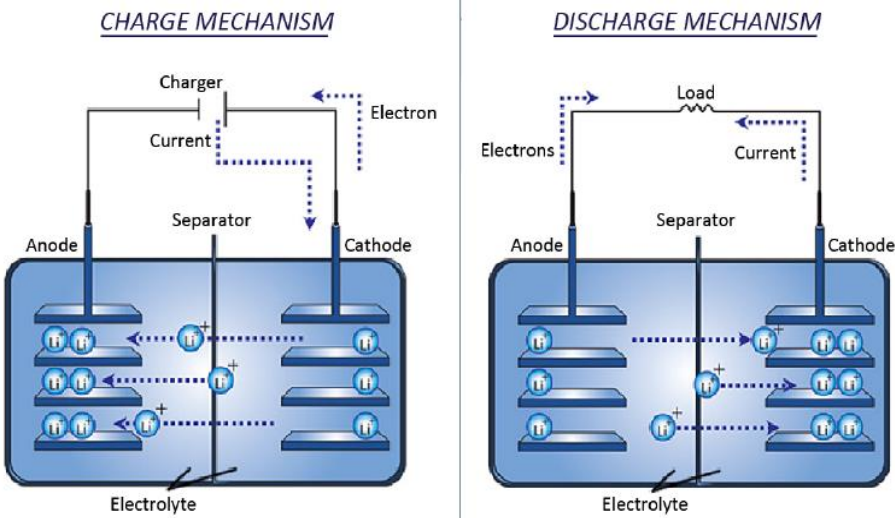
Figure 2.6: Charging and discharging phase of a battery

The electrons can't go back to the anode because of the electro neutrality due to the simultaneous ions movement inside the electrolyte. The porous septum avoids the mixing of the solutions and guarantees the passage of ions and electrons through two different ways.

Without the porous septum, there would be a short circuit with electrons going from anode to cathode without passing through the external circuits.

The useful effect depends on the number of electrons exchanged between the two electrodes. The reverse process is made possible thanks to an external electrical field that reverses the way of the electrons bringing the system back to the initial state.

This working principle allows to create an energy storage system.

2.1.1 POLARIZATION EFFECTS IN BATTERIES

The voltage of the battery depends on the difference of electrochemical potentials between the oxidation and reduction reactions. The voltage of the battery ΔE^0 can be calculated as:

$$\Delta E^0 = \frac{-\Delta G_r^0}{zF} \qquad (2\text{-}1)$$

Where ΔG_r^0 is the Gibbs free energy in standard conditions, z is the number of electrons involved in the reaction and F is the Faraday constant equal to 96485.64 C.

The initial voltage of the battery is the one in ideal and equilibrium conditions that is the one with the battery disconnected from the load. When the equilibrium is broken, the voltage can greatly vary with deviations proportional to the rate of charge and discharge. These deviations are known as *polarization effects*. There are three main polarization mechanism:

- *Kinetic overvoltage,* that is the voltage needed to break the equilibrium and activate the electrochemical reactions

- *Ohmic overvoltage,* due to resistive loss in the battery. These losses are connected with the resistance to the electronic motion in the external circuit and to the ions in the electrolyte. They follow a linear trend according to the Ohm law:

$$\Delta V = RI \tag{2-2}$$

Where ΔV $[V]$ is the potential difference between anode and cathode, R $[\Omega]$ is the internal resistance and I $[A]$ is the current.

- *Overvoltage due to mass transport*, particularly influent for high charge rates and discharge rates. During the discharge phase, the concentration of the reacting species around the electrode drops down making the voltage of the battery decrease faster than the equilibrium conditions. Vice versa, in the charging phase, there is a higher concentration of the reacting species around the electrode, with a value of the voltage higher with respect to the ideal case. The overvoltage due to mass transport impacts negatively on the battery capacity because some reacting species are not used when the minimum safety voltage is reached thus limiting the capacity of the battery at disposition. The main effect of this kind of overvoltage is the limitation of the charge and discharge currents.

Other phenomena provoking the detachment from the ideal conditions are the parasitic reactions which take place inside the battery. These reactions, during the discharge phase, use some electrons which should be sent to the load, vice versa during the charging phase they use some charges that should be used to recover the initial conditions of the electrodes.

2.1.2 BATTERY TECHNICAL PARAMETERS

Following, a brief description of the main parameters useful to match different kind of batteries is given [15] [16] [17] [18].

Voltage [V]: potential difference inside the battery determined by the chemical reactions, by the concentration of reacting species and by polarisation. The nominal voltage cannot be measured directly but it is approximated to the one measured at open circuit.

Cut off voltage [V]: potential difference under which the battery can no more be discharged in order to avoid permanent damages.

Capacity [Ah]: The amount of the charge that can be extracted from the battery until the minimum value of voltage is reached. It depends from the discharge current and from the temperature.

State of Charge (SOC) [%]: the amount of energy inside the battery with respect to the total available one.

Depth of Discharge (DOD) [%]: maximum amount of energy that can be extracted from the battery with respect to the total available one.

Monthly Self Discharge [%]: phenomenon provoked by the lack of battery use, which tend to gradually lose the energy content inside them. Self-discharge is due to corrosion and impurities in the electrolytes, insulation defects or high internal resistance.

Specific Energy [Wh/kg] and Energy Density [Wh/m^3]: it is the energy that can be stored with reference to weight and to volume.

Specific Power [W/kg] and Power Density [W/m^3]: it is the power of the battery referred to its weight and to its volume.

Energy efficiency [-]: ratio between the extracted energy and the one used to bring the SOC back to the initial state.

Coulomb Efficiency [-]: ratio between the charges entering the battery during the charging phase and the charges extracted during the discharging phase.

Number of charging/discharging cycles [-]: parameter used to estimate the life of a storage system. It represents the number of complete charging and discharging cycles that a battery is able to achieve before its performances drop below a minimum limit (typically before a reduction of 20% in its capacity). Its value is dependent from the DOD and from the working conditions.

2.1.3 MAIN KINDS OF BATTERIES

Next, a description of the main kinds of batteries is given in order to understand their main advantages and drawbacks.

<u>Lead Acid Batteries</u>

This kind of batteries is the most widespread in the world due to its low cost and the easiness to find its raw materials. They are used in UPS, telecommunications and emergency feeding [17]. The positive electrode is made of a lead oxide whereas the negative one is made of lead. Both the electrodes are submerged in a solution of sulphuric acid that participates to the redox reactions. The electrolytic solution is only used to enable the ion transport.

The total reaction inside the battery is the following:

$$PbO_2 + Pb + 2H_2SO_4 \leftrightarrow 2PbSO_4 + 2H_2O \tag{2-3}$$
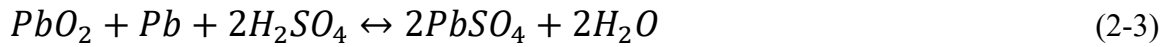
The standard potential difference for one cell is 2.048 V [17]. This value must not be exceeded to avoid water electrolysis with the undesired formation of hydrogen at the negative electrode and oxygen at the positive electrode. This phenomenon provokes the reduction of charging efficiency since part of the charging current is used in the parasitic reaction and an increase in the self-discharge rate.

The most of these batteries are made of a series of cells with the alternation of flat positive and negative layer, where a very thin active coating is applied on grid made of lead alloy for receiving the current.
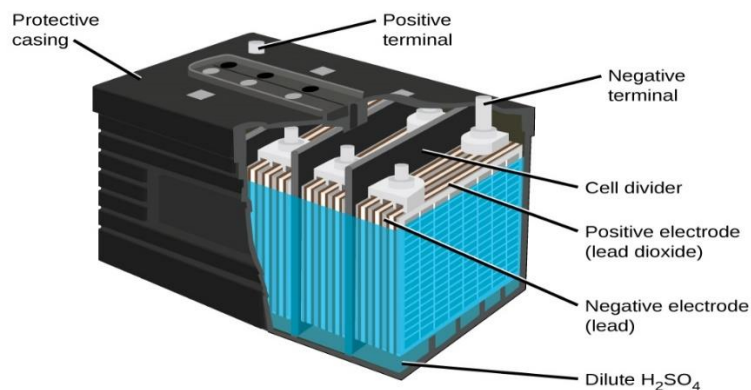
Figure 2.7: internal structure of a lead acid battery

An important problem related to the positive grid is the corrosion provoked by the overcharge which damages structurally the battery and in the worst case it makes it not usable any more. To avoid this, some special controls of the battery SOC have been implemented. The state of charge of these batteries is easily calculated by measuring the variation of the electrolyte density

after water formation taking into account the lower specific weight of water with respect to the sulphuric acid.

Another problem of this kind of batteries is the sulphation which is a common phenomenon when working at partial charge (for example when considering the integration of battery with intermittent RES). During discharge, lead sulphate is produced and it accumulates over the negative electrode. If the discharge is very deep, $PbSO_4$ crystals increase their sizes not participating to the following reactions any more and provoking serious damages to the battery. To increase battery life, it is necessary to recharge it with not too high currents.

The energy efficiency of lead acid batteries is around 70% even if it increases when the rate of charge and discharge decrease and when temperature increases. Instead, the Coulomb efficiency is equal to 85%. For energy storage applications the other technical characteristics are:

- Specific energy equal to 25-40 Wh/kg

- Specific power equal to 100-500 W/kg

- Energy density equal to 40-100 kWh/m^3

- Power density equal to 400-600 kW/m^3

With a correct use of this battery, the battery can last up to 15 years with costs which are the lowest in the energy storage scenario [16].

<u>Lithium Ion Batteries</u>

Thanks to their performances, lithium ion batteries are used in nearly every kind of portable application. They can be also used in automotive applications and in energy storage systems

both on small and large scale. Lithium is one of the lightest metals with a high electrochemical potential so that it is suitable for batteries with high energy density and high power density.

The negative electrode of this kind of battery is made of graphite whereas the positive one is a lithiate oxide of a transition metal. The electrolyte instead is a lithium salt submerged in an organic solution. When the cell is completely discharged, all the lithium can be found in the cathode. During the charging process, lithium ion are extracted from the metal oxide and transferred to the anode whereas the electrons migrate from cathode to anode through the external circuit. The charging process determine the encaging of the ions in the graphite matrix with the acquisition of electrons coming from the external circuit. During the discharge, the reverse process occurs which brings back the system to its initial conditions.

The generic reaction is:

$$C_6Li_x + Li_{(1-x)}MO_2 \leftrightarrow 6C + LiMO_2 \qquad (2\text{-}4)$$
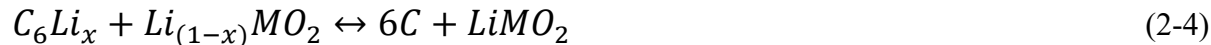
Where x is the number of available sites for lithium ions in the anode structure and M is a generic metal. The choice of the metal is fundamental since it determines the maximum allowable potential difference. The cells available in the market have a voltage of about 3.7 V and a cut off voltage of 2.7 V. An important problem typical of lithium ion batteries is the formation of a passivating layer made of oxides, carbonate hydroxides and fluorites between the electrolyte and the negative electrode, called SEI (*solid electrolyte interface*). This creates after the first charging cycle and causes a loss of 10% in the capacity because it contrasts the diffusion process of ions; as the number of cycles increases, this layer tends to stabilize after a further reduction in the capacity. Other problems are related to the continuous problems of intercalations and de intercalations that provoke, as time goes by, structural deformations in the

cell. Finally, it is to underline the sensitiveness of these cells to electrical and thermal overload conditions. Because of this fact it is necessary to adopt a suitable system for cell voltages balancing and a *BMS (Battery Management System)* able to intervene in abnormal conditions. Lithium ion batteries differentiates even for anodic and cathodic materials. The anode is nearly always in graphite whereas the cathode can be made with several kinds of metal oxides. The first cathodic material to be adopted was the lithiate oxide of cobalt ($LiCoO_2$) characterized by a great chemical stability and by a good possibility to store lithium ions. These material has also some cons since it is toxic and expensive and the overcharging phase of the cell has some problems with the risk to damage the structure of the material itself. Another alternative consists in the creation of cathodes made of mixed oxides, using three transition elements. Nickel-Cobalt elements are widespread such as $LiNi_{0.8}Co_{0.15}Al_{0.05}O_2$ (NCA) and $LiNi_{0.33}Mn_{0.33}Co_{0.33}O_2$ (NMC) which allow to get better performances with lower prices. Another kind of cathodes is made of lithium/manganese compounds $LiMn_2O_4$ which have a better thermal stability. In the las few years even the lithiate phosphate of iron has become more and more widespread thanks to its low cost and its higher safety with respect to other kinds of metal oxides. Unfortunately, this technology has a low ionic conductivity.
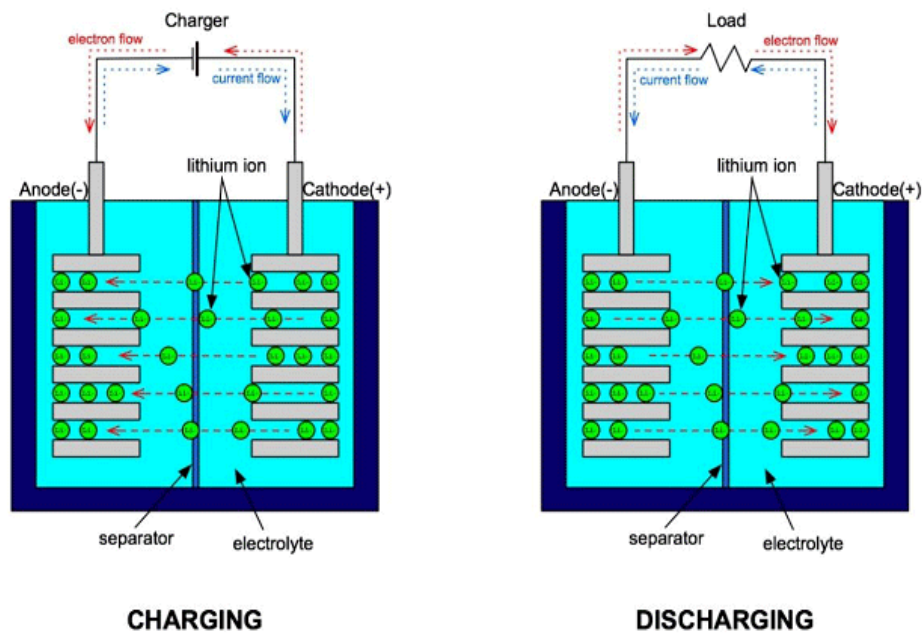
Figure 2.8: Charging and discharging phase for a lithium ion battery

Coulomb efficiency is low due to the absence of parasitic reactions. The round-trip one is particularly high with values of 90% or more. The discharge can reach the totality of the battery capacity and the power can be released with a DOD of 80%. The self-discharge rate is about 1% per month. The main problems related to this kind of batteries are the solvents inside the liquid electrolytes, which can be corrosive or flammable [23] [24].

Sodium/sulphur batteries

Sodium sulphur batteries are batteries that work at high temperature with two melted electrodes. A ceramic separator allows the passage of ions working as an electrolyte. The cathode is made of liquid sulphur, the anode instead by sodium in liquid state. The ceramic separator made of β''-alumina (beta prime prime alumina) allows ion to pass only at temperatures near 300°C and because of this need and the need for electrodes to be in molten state the temperature has to remain high during cell operation. Because of the corrosive power of liquid sulphur, the cathode

current collector has to be made of precious alloys based on materials such as molybdenum or chromium.
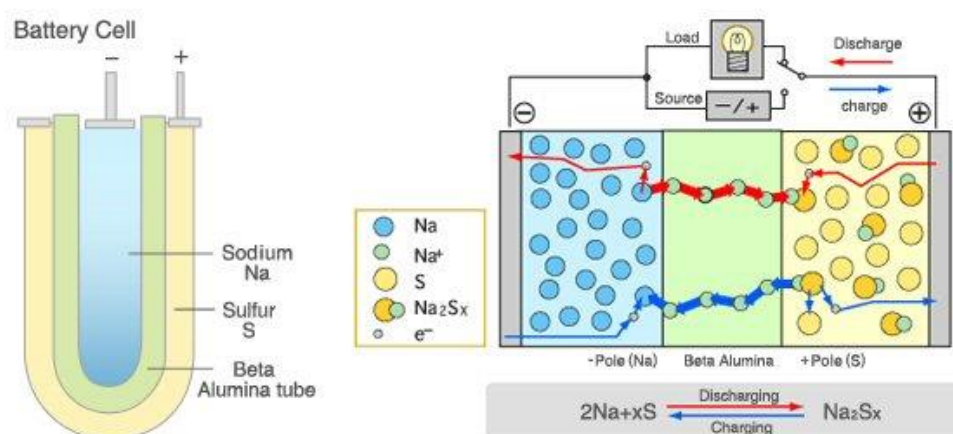
Figure 2.9: Structure and working principle of sodium/sulphur battery

Redox Vanadium flow batteries

In this kind of batteries, the active materials are in the form of two redox coupled solutions, melted in ionic form inside the liquid electrolyte and stored into external vessels, where they are pumped inside the electrochemical cell and kept separated through the interposition of a membrane. The membrane is generally made of NAFION which is suitable for cationic transport. Thanks to the separated vessels it is possible to decouple power and capacity; the absorbed or generated power depends on the quantity of the electrolyte that participates to the reaction. The storage capacity depends on the amount of electrolyte stored inside the vessels. In Vanadium batteries, the redox couple is constituted by V^{2+}/V^{3+} at the positive electrode

whereas the valence state +4 and +5 exists at the negative electrode in the form of VO^{2+} and VO_2^+ inside a solution of sulphuric acid. The two redox reaction that occur are:

1) $V^{2+} \leftrightarrow V^{3+} + e^-$ (2-5)

2) $VO^{2+} + H_2O \leftrightarrow VO_2^+ + e^- + 2H^+$ (2-6)
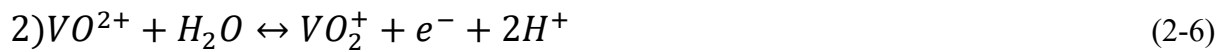
The oxidation of V^{2+} to V^{3+} creates a potential of 0.255 V whereas the oxidation from V^{4+} to V^{5+} creates a potential 1.004 V with the simultaneous separation of water molecule which determines the release of hydrogen ion exchanged between the two electrolytic solution through the separation membrane. The final standard cell potential is of 1.259 V.

The vanadium flow batteries have a low energy density because of the low solubility of vanadium salts. The theoretical limit is 65 Wh/kg.

The high cost of these batteries can be reduced by adopting large size systems suitable to applications which generate energy.
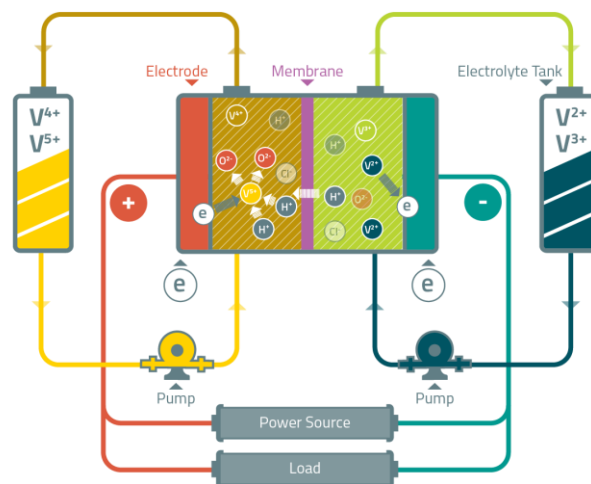

Figure 2.10: Vanadium flow battery

2.2 GOALS OF ENERGY STORAGE

The integration of storage system with a PV plant can generate environmental, operational and financial benefits both to the utilities and to the customers thanks to measures such as *peak shaving, load shifting, grid support* and *demand response.*

The aim of peak shaving is to minimize the energy demand for residential customer or to reduce peak loads that utilities have to face. In this case, the storage device has to provide the necessary power above a certain threshold when PV is not available. Peak shaving failure can have a bad consequence on customers' rates based on monthly peak demand.

Load shifting instead is useful when customers purchase utility power on a time of use basis. Unfortunately, peak loads are not matched by PV generation peaks. By integrating a PV system and a storage system, it is possible to decrease the demand of utility power during late-day periods charging the storage early in the day to face a load later in the day.

Thanks to demand-response the utility is able to control high load devices such as heating, ventilation, air conditioning and water heating with progressing operations during high demand periods. If the PV storage system is correctly sized, the implementation of demand response strategy should have little or no effect on local operations. A one way communication between the PV storage site and the utility is necessary for control system to perform demand response correctly. Three options for demand-response are available: *direct load control (DLC), voluntary load reduction and dynamic demand*. Thanks to DLC, utilities have the control on selected customer load under contracts providing compensation to the customer. In some cases, grid operators can decide to turn on customer load or to recharge storage systems during time of low system load avoiding to make central power plants work below minimum allowable values. DLC reduce customer autonomy but offer utilities the possibility to reduce the loads

when needed. Voluntary load reduction, instead, send signals to customers to persuade them to reduce their electrical consumption.

This can be done with on/off signals promising a future economical compensation or with a time-linked electricity price signal with high prices used to discourage electricity usage and low prices to encourage it. Similarly to DLC, customers can choose between comfort and economic convenience but they can be more autonomous. Dynamic demand is a less common demand response technique in which loads adjust their start and stop in order to stabilise grid frequency compensating customers who implement it.

Another option of storage is the power supply to residential or commercial customers during outages that is when utility is not able to produce power. To do this, residential customers have to be intentionally islanded from the utility. Safety regulations were created to avoid the back feeding on transmission and distribution lines during islanding or black out. Islanding is useful both for the utility and for the customer because it allows to reduce loads during high demand periods and to satisfy the customer's loads in case of fault of the utility.

Finally, energy storage can be a useful way to improve grid power quality with the possibility to regulate bus voltages, adjust phase angles and eliminate harmonic distortions from electrical grid. Traditionally, this function is supplied by the UPS devices on the customer side. UPS are able to correct AC power deviations within milliseconds. Furthermore, the improvement in grid power quality, due to battery-integrated PV, can be noticed in reactive power compensation and harmonic cancellation. *[19] [20]*

2.3 SMART GRIDS

A *Smart Grid* is the combination of an information grid and a distribution grid which allows a smarter management of energy distribution minimising possible overloads and variations of electric voltage around its nominal value. This concept implies a strong presence of distributed generation even of small size located in the peripheral nodes of the distribution grid which are generally designed for unidirectional energy flows. Due to the aleatory of renewable sources such as wind and solar, the distributed generation has to manage locally possible surplus of energy addressing them to contiguous areas in which there is an energy deficit constantly regulating the production of centralized power plants connected to the national transmission grid. Smart grids are regulated with software designed to check the information thanks to monitoring system which take into account the whole electric flux and which allow to integrate renewable energy in the system. When the energy price becomes low, a smart grid can also decide to activate industrial processes or home appliance systems. [21] [22]

The creation of a smart grid is a complex process but national governments are addressing their efforts to the improvement of these innovative distribution system. At this moment, it is possible to distinguish peak hours from off-peak hours with higher prices when energy is consumed during peak hours and lower prices when energy consumption is concentrated during off peak hours. Thanks to particular routers, a smart grid can perform an optimal energy balance, provide a data band with very low management costs, find energy islands on national and continental scale and finally integrate in a *Home area network* to allow a smart interaction of home appliances.
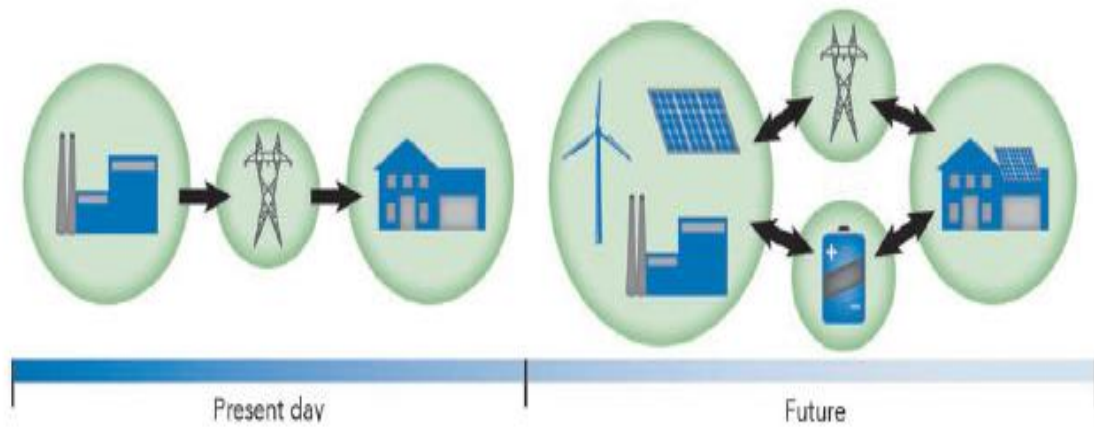
Figure 2.11: Present and future energy flows

A smart grid has with embedded real time sensors is able to achieve a self-restoration avoiding problems related with over currents or energy interruption. The system has to be able to foresee possible faults and find efficient strategies to face them. Consumers can benefit of an energy cost reduction deriving from a correct management of the smart grid and of a certain easiness in injecting renewable energy into the grid. Another important function of the smart grid is the ability to recognize manual interruption of the electrical supply readdressing the energy flux elsewhere. With this kind of distribution system the voltage remains stable and its oscillations are then reduced thus decreasing the high costs associated to perform this task. Losses associated with energy transportation are reduced since the consumption of local energy production is incentivized but this makes protection systems more intrinsic complex since they have to be able to distinguish faults from energy withdrawal. *[21]*

2.4 NOTES ON SMART METERS

A particular equipment called *smart meter* is able to continuously monitor the power absorbed or injected into the grid. An important task of the meter is to make sure that the maximum contract power is not exceeded. Unlike conventional electricity meters, smart meters are capable of two way communication with the utility and to measure electrical consumption with high time resolution (typically with one hour interval). Besides, smart meters are able to communicate energy usage back to the utility regularly even with a real time transmission. Communication occurs through various tools including also Internet, radio, Wi-Fi, cell modem or satellites. Information from the utility can be made of price signals, connect/disconnect signals or DR information. The adoption of smart meters enables advanced electricity pricing scheme improving the profitability of distributed photovoltaic and also the activation of DR scheme which are synergistic with PV installations. Some of the most advanced smart meters are able to measure data about power quality, power outages, power factor, reactive power usage and grid voltage and frequency. The payback time of a smart meter range between three to ten years. A benefit for utilities is that they are no longer obliged to send workers out to read meters. This is possible also with *automatic meter reading (AMR)* systems that do not involve the use of smart meters. If AMR is already installed, the payback of smart meter is not ensured whereas it is convenient to install a next generation meters if AMR has not been implemented. Finally, an important task for utilities is to evaluate carefully the flexibility and upgradability of smart meters before installation.

CHAPTER 3: BATTERY MANAGEMENT SYSTEMS

The topic of *Battery Management Systems (BMS)* is becoming more and more popular in energy engineering literature. The main purposes are the improvement in self-consumption and so the use the excess of solar energy during evening and night periods and the minimization of maximum power exchanged with the grid. Another important matter is the size reduction of this electrochemical devices since their cost is still high and this negatively affects the investment cost. An intelligent battery energy management has to face these problems by discharging the battery when it is more necessary and eventually taking into account the electricity price over the whole day or weather conditions. In the next paragraph, some examples of BMS are illustrated and finally the proposed BMS taking into account the day ahead energy balance is described.

3.1 BATTERY SIMULATION ACCORDING TO STANDARD BMS

In the standard BMS, the working mechanism of battery is simulated according to an energy model based exclusively on power flows entering and exiting the system without considering a series of factors about current, voltage and variation of charging efficiency with temperature and state of charge. Besides, also self-discharge phenomenon and reduction of battery capacity have not been taken under consideration.

The inputs of the model are:

- The difference between the PV power output and the load at time t, $P_{PV}(t) - P_{LOAD}(t)$ [kW]

- The minimum state of charge which is supposed equal to 0.2

- The SOC at the considered instant, which is equal to 1 at the beginning of the simulation (this means that the battery is fully charged when simulation starts)

- The charging efficiency η_{ch} equal to 0.9

- The maximum power that the battery can absorb from PV or provide to the load $P_{battmax}$ [kW]

- The maximum capacity of the battery C_{batt} [kWh]

In order to get better and more realistic results, the simulations are minute by minute simulations which are able to highlight sudden variations in PV generation and in the power absorbed by the load.

Charging phase

When charging the battery, the first thing to do is to make sure that the difference between PV power output and the load at time t, that is $P_{batt}(t)$, does not exceed the maximum limit allowed for the battery $P_{battmax}$. If this happens, the excess of energy with respect to $P_{battmax}$ is sold to the grid avoiding its dissipation. Then the battery state of charge is evaluated according to the following formula:

$$SOC(t) = SOC(t-1) + \frac{P_{batt}(t)\Delta t \eta_{ch}}{C_{batt}} \tag{3-1}$$

Where $SOC(t-1)$ and $SOC(t)$ are the initial and final state of charge of the considered iteration.

If $SOC(t)$ exceeds the unit, the battery will not be able to absorb the whole input power. So the battery will absorb power until its SOC reaches the value of 1 injecting into the grid the remaining part of power.

In this case the total power that the battery will absorb, $P_{batt}(t)$, will be equal to:

$$P_{batt}(t) = (1 - SOC(t-1))C_{batt}\frac{1}{\eta_{ch}\Delta t} \tag{3-2}$$

$P_{grid}(t)$ (kW) represents the amount of power sold to the grid: in some cases, it can be equal to the amount of power that exceeds $P_{battmax}$ plus the power that the battery cannot store any more due to the reaching of the full charge. The charging process can be fully summarized in the flow chart in figure 3.1.
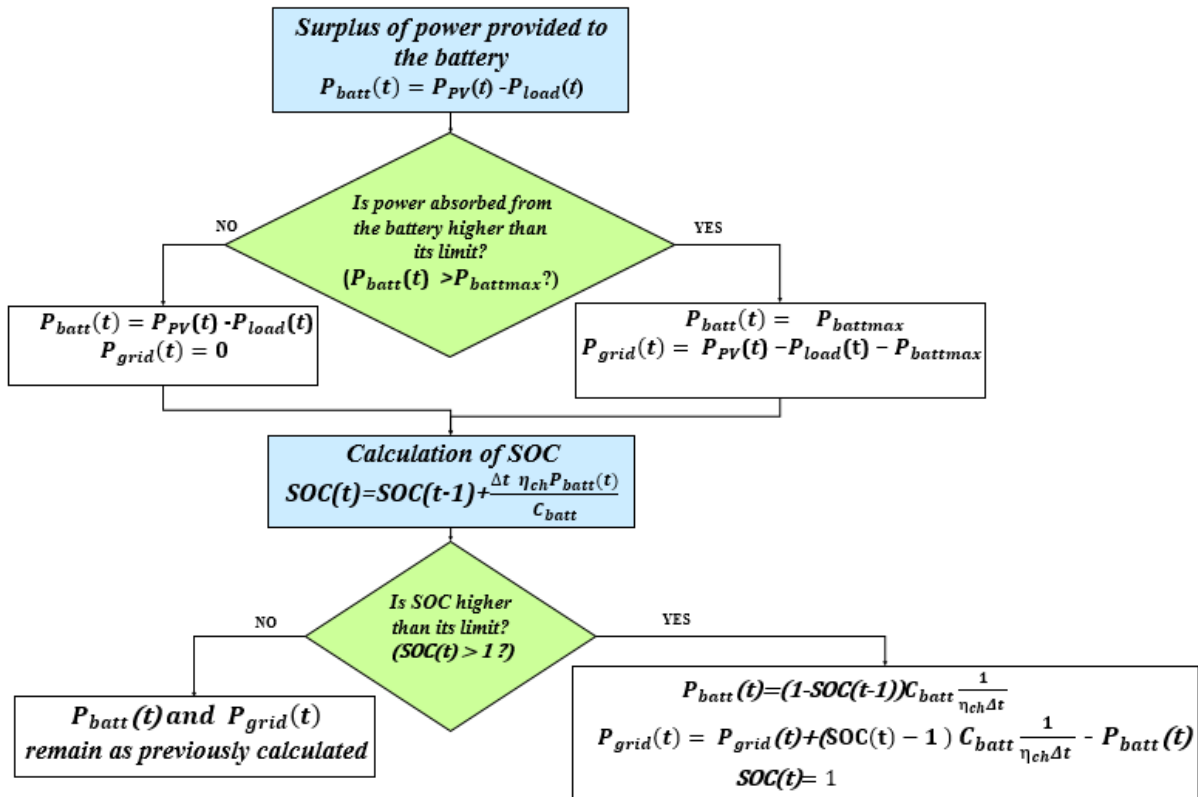

Figure 3.1: Standard battery charging process

Discharging phase

During discharging process, the first thing to do is to check if the difference between PV generation and the load at time t is lower than $-P_{battmax}$. If this happens, the power bought from the grid will be equal to $P_{PV}(t) - P_{LOAD}(t) + P_{battmax}$. Again, the battery state of charge is calculated as:

$$SOC(t) = SOC(t - 1) + \frac{P_{batt}\Delta t}{C_{batt}} \qquad (3\text{-}3)$$

If SOC(t) goes below 0.2, the battery will not provide power any more. In this case, the battery will provide power until its SOC reaches 0.2 then the extra power will be provided by the grid. The total amount of power provided by the battery, $P_{batt}(t)$, can be expressed as:

$$P_{batt}(t) = (0.2 - SOC(t - 1))\frac{C_{batt}}{\Delta t} \qquad (3\text{-}4)$$

$P_{grid}(t)$ (kW) stands for the total amount of power bought from the grid: in some cases, it can be equal to the amount of power that exceeds $-P_{battmax}$ plus the power that the battery cannot provide any more due to the reaching of the full discharge. Similarly to the charging process, the discharging process can be fully summarized in the flow chart in figure 3.2.
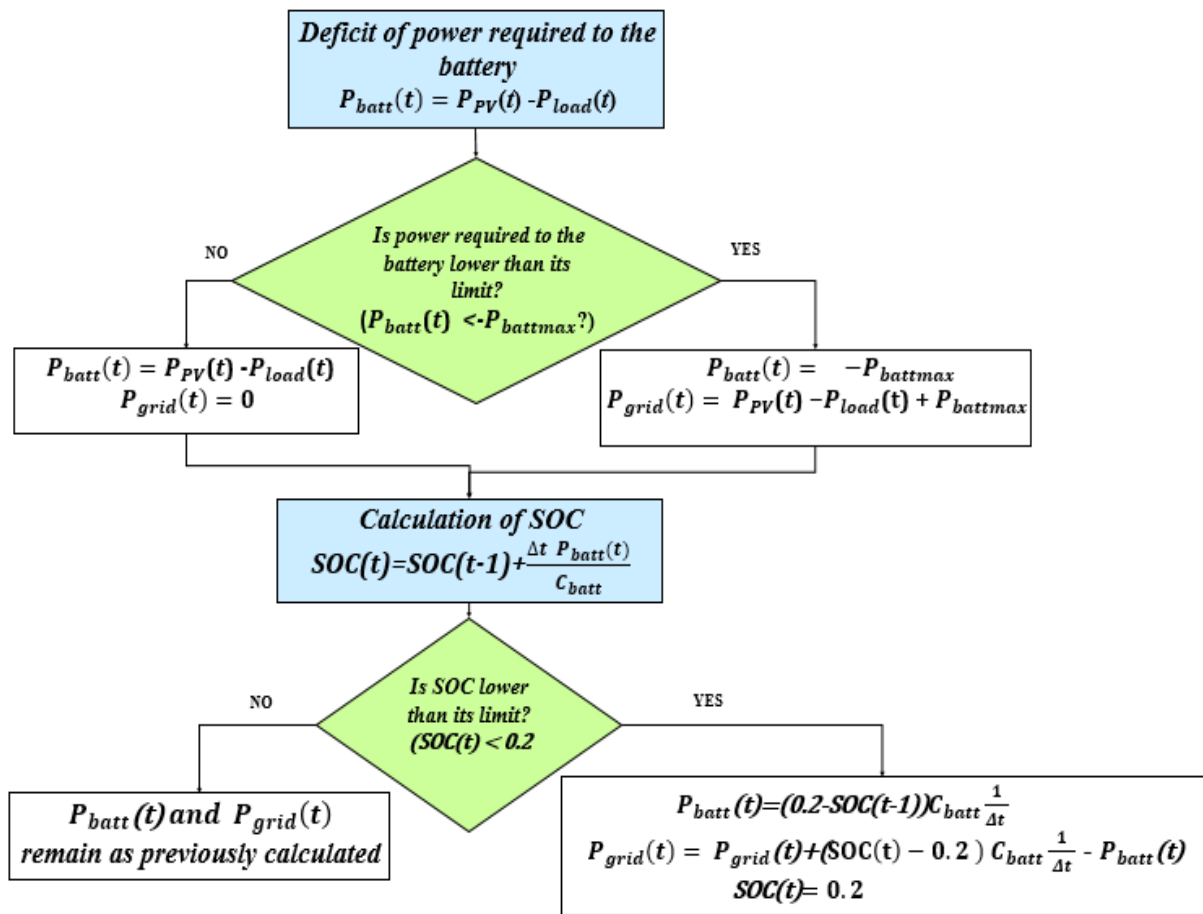
Figure 3.2: Standard battery discharging process

3.2 BATTERY MANAGEMENT SYSTEMS DISCUSSED IN ENGINEERING LITERATURE

The two paragraphs below are about two Battery Management Systems found in literature. The first one, published in the article [25], aims to maximize self-consumption by considering the difference between real and predicted PV power output making use of quadratic programming to minimize power bought from the grid. The second one, in the article [26], makes the battery work as a 'power smoother' thus reducing fluctuations in PV power output and creating a benefit for the grid which receives a more constant power profile from the PV plant.

3.2.1 BMS FOR MAXIMIZATION OF SELF CONSUMPTION USING QUADRATIC PROGRAMMING

The described strategy takes into account the difference between the real and predicted power output of photovoltaic. The actual generated PV power can deviate from predictions because of passing clouds or possible system faults. The feasibility of this scheme is applied to a small system which is made of a PV generator, a battery for energy storage and a grid/load connection. This scheme reduces variation in the state of charge (SOC) of the battery and minimize grid utilisation in function of the difference between the actual and predicted power.

At each moment the energy balance equation is written as:

$$P_{Load}(t) = P_{PV}(t) + P_{Grid}(t) + P_{Batt}(t) \tag{3-5}$$

Where $P_{Load}(kW)$ is the power demand from load, $P_{Grid}(kW)$ is the power provided by the grid, $P_{PV}(kW)$ is the power output of the PV generator and $P_{Batt}(kW)$ is the power exiting or entering the battery.

Using quadratic programming the minimisation problem over time $\sum_{t=0}^{\infty} ||P_{Grid}||_2^2$ can be converted into $\sum_{t=0}^{\infty} ||P_{Load} - P_{PV} - P_{Batt}||_2^2$. This problem is simplified using some assumptions which are:

- Charge and discharge of the battery are considered to be identical

- The estimation of PV power is provided by weather forecast

- The power consumed by the load P_{Load} is known

In order to compensate for the difference between the measured and estimated PV output power, a *scaling factor* is calculated at each time interval t. The scaling factor is defined as:

$$\alpha_t = \frac{P_{PV}^{real}(t) + P_{PV}^{real}(t-1)}{P_{PV}(t) + P_{PV}(t-1)} \tag{3-6}$$

The scaling factor varies between 0 and 1 and it is 1 when the denominator goes to zero.

By considering α_t, the value of the power of the battery which minimizes the power absorbed from grid can be written as:

$$P_{Batt}(t, SOC_t, P_{PV}, P_{Load}) = \arg\min_{Pbatt} \sum_{k=t}^{t+N_h-1} ||P_{Load} - \alpha_t P_{PV} - P_{Batt}||_2^2 \tag{3-7}$$

The constraints of the problem which have to be adopted are:

- $SOC_{min} \leq SOC \leq SOC_{max}$ that is the state of charge does not have to exceed the maximum or go below the minimum

- $P_{Batt}^{min} \leq P_{Batt} \leq P_{Batt}^{max}$ which means that the power of the battery is limited between a maximum value and a minimum value

This scheme analyses the amount of power given by the grid over a wide range of scaling factors. For example, a scaling factor of 0.7 means that PV output power is reduced by

(1-α_t)100=30%. It is possible to notice that energy drawn from the grid reduces as the scaling factor increases.

The improvement in performance is evident when considering the difference between the scheme which accounts for the scaling factor and the scheme which does not make use of it.

The improvement, however, reduces as α_t increases because for higher values the system cannot allow further improvements. Consequently, with high values of the scaling factor the conventional and the proposed scheme seem to converge. Another aspect to take under consideration is the time interval. With a reduced sampling time, the energy given by the grid is higher because of the increased energy intake by the battery. Besides with a shorter sampling time the accuracy of predictions improves highlighting larger variations in the scaling factor and in the PV output power.

3.2.2 BMS FOR CONSTANT PHOTOVOLTAIC PRODUCTION

This kind of BMS is suitable in cases of high penetration of distributed PV generation into a smart grid. It is important that the power injected into the grid by solar panels is as constant as possible in order to allow the grid to work without any problems. Thanks to the storage system, it is possible to smooth solar power output to compensate fluctuations that derive from passing clouds and from variation in solar radiation. Another advantage is the possibility to control the voltage at the point of common coupling.

In this case, at each time interval, the following equation has to be satisfied:

$$\sum_t P_{PV-smooth-ref}(t) = \sum_t P_{PV} + \sum_t P_{Batt} \qquad (3\text{-}8)$$

Where $P_{PV-smooth-ref}(kW)$ is the reference smooth PV profile, $P_{PV}(kW)$ is the PV power and $P_{Batt}(kW)$ is the battery power.

The idea behind this management is that the battery recharges when the PV output power exceeds the reference smoothed PV power and discharges when the PV output power goes below the reference smoothed PV power. In this way, it is possible to maintain a constant PV output power which does not interfere with the grid. Thanks to this BMS, plant owners can increase their profit by selling more power to the grid especially during sunny summer days when PV production is high. An important goal to achieve is to maintain a constant PV output power even during long periods of passing clouds which may happen during winter season.

3.3 NOTES ON FORECAST OF PV PRODUCTION

In order to make a forecast of the PV production, it is necessary to rely on weather forecast. Thanks to an Internet connection, the inverter is able to know in advance the weather forecast of the following day. Once known the forecast and the current month, the inverter selects a suitable irradiance profile using the software PVGIS.
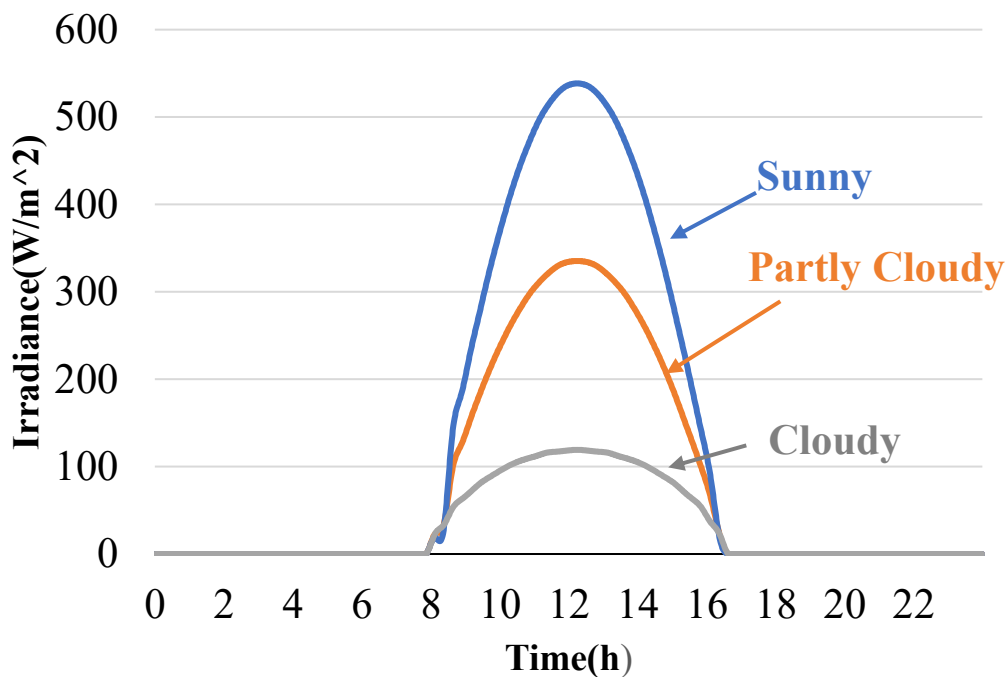

Figure 3.3: Behaviour of irradiance during the month of December in Turin

From the irradiance and the ambient temperature, it is possible to calculate the forecasted PV power output according to a selected weather condition. To do this a model of the PV generator is applied. This model considers several losses which reduce the conversion efficiency. These losses are:

- **Temperature losses** l_{th}: due to the reduction of the electrical potential of the PV cell when temperature increases. For the PV modules adopted, l_{th} is supposed to be equal

to 0.34%/°C. This factor estimates every minute the loss caused by the difference between the temperature cell (T_c) and the STC condition (T_{STC}).

$$l_{th} = \gamma_{th} \cdot (T_c - T_{STC}) \tag{3-9}$$

The temperature of the cell T_c is calculated with the following equation:

$$T_C = T_{amb} + \frac{NOCT - 20}{0.8 \left[\frac{kW}{m^2}\right]} \cdot G \tag{3-10}$$

Where:

- T_{amb} is the ambient temperature [°C]

- NOCT (Normal Operating Cell Temperature), supposed equal to 47°C;

- 0.8 is the value of irradiance in NOCT condition;

- G is the value of irradiance provided by the software PVGIS [kW/m²].

- **Losses due to mismatch η_{mis}** due to possible non uniformities in the cells: it may happen that a cell have the I-V curve different from the others because of a defect in manufacturing or phenomena of partial shading. This provokes a reduction of the PV generator performances which are subjected to the faulty cell. These losses cannot be avoided due to the connection in series or in parallel of the several cells to increase voltage and current. η_{mis} is supposed to be equal to 0.97.

- **Ohmic losses η_{cab}** due to the dissipation of electrical energy in the form of heat (Joule effect). Generally they depend on the section and on the length of the cables. These losses are supposed to be equal to 0.99.

- **Losses due to dust η_{dust}** which are kept to a reasonable value thanks to the periodic cleaning of the frontal glass. This kind of loss is high near pit. In this case they are supposed equal to 0.976.

- **Reflection losses η_{refl},** due to solar radiation that is reflected from the glass which protects the cells. The interposition of the glass is necessary because without it the most of solar radiation would be reemitted in atmosphere as infrared radiation causing higher losses. The value of η_{refl} is assumed to be equal to 0.973.

For the sake of simplicity, the efficiency of the DC/DC converter (MPPT) is supposed to be equal to 1. Knowing all these parameters and the inverter efficiency (equal to 0.968), it is possible to forecast the AC PV power output $P_{PV,AC}$ with the different weather conditions.

$$P_{PV,AC} = PV_{nom} \cdot \frac{G}{1000} \cdot \left(\eta_{dust} \cdot \eta_{refl} \cdot \eta_{mis} \cdot \eta_{cab} \cdot \eta_{inv}\right) \cdot (1 + l_{th}) \qquad (3\text{-}11)$$

Where PV_{nom} stands for the nominal power of the PV generator [kWp].
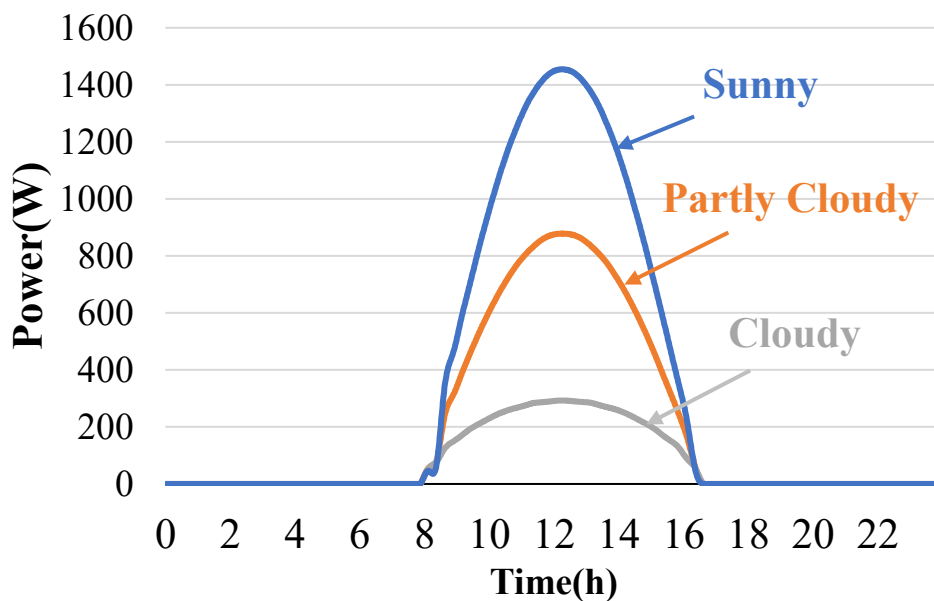

Figure 3.4: Expected AC PV power output in December (Turin)

3.4   PROPOSED   BMS   ACCOUNTING   FOR FORECASTED ENERGY BALANCE

The aim of the proposed BMS, object of this thesis, is to minimize the maximum power absorbed from the grid by taking into account the forecasted energy balance in selected time slots. This BMS divides the day into three periods:

- 0AM-6AM

- 6AM-6PM

- 6PM-12PM

The energy balance in the selected time slot is calculated as the difference between the PV energy production and the energy consumed by the load. The time slot which goes from 6AM to 6PM identifies the period in which the most of PV power is generated throughout the year. Generally during the first and especially the last time slot the energy consumed by the load, due to the presence of evening peaks, is higher than PV production. The energy balance during 0AM-6AM and 6PM-12PM is surely negative on winter period when the small amount of PV generation is concentrated only in the second time slot.

Time slot	Energy balance (E_{PV}-E_{LOAD})			
	01-Dec	02-Dec	03-Dec	04-Dec
0:00AM-6:00AM (kWh)	-0.7	-0.5	-0.6	-0.5
6:00AM-6:00PM (kWh)	3.6	2.9	-2.8	0.9
6:00PM-12:00PM (kWh)	-0.9	-0.9	-1.7	-2.6

Table 3.1: Energy balance in the three daily time slots in the first four days of December

According to the next day energy balance, it is possible to control the amount of energy which can be drawn from the battery during the current day and the one that has to be left inside the battery thus achieving a more rational use of energy. In this way, it is even possible to reduce the size of the battery with consequent economic savings.

The integration of the proposed BMS inside the inverter allows the battery to perform the several operations such as Peak Shaving or energy distribution in more time slots.

For a deeper comprehension of this BMS, the flow chart in figure 3.5 is used to explain all the possible cases which may occur.
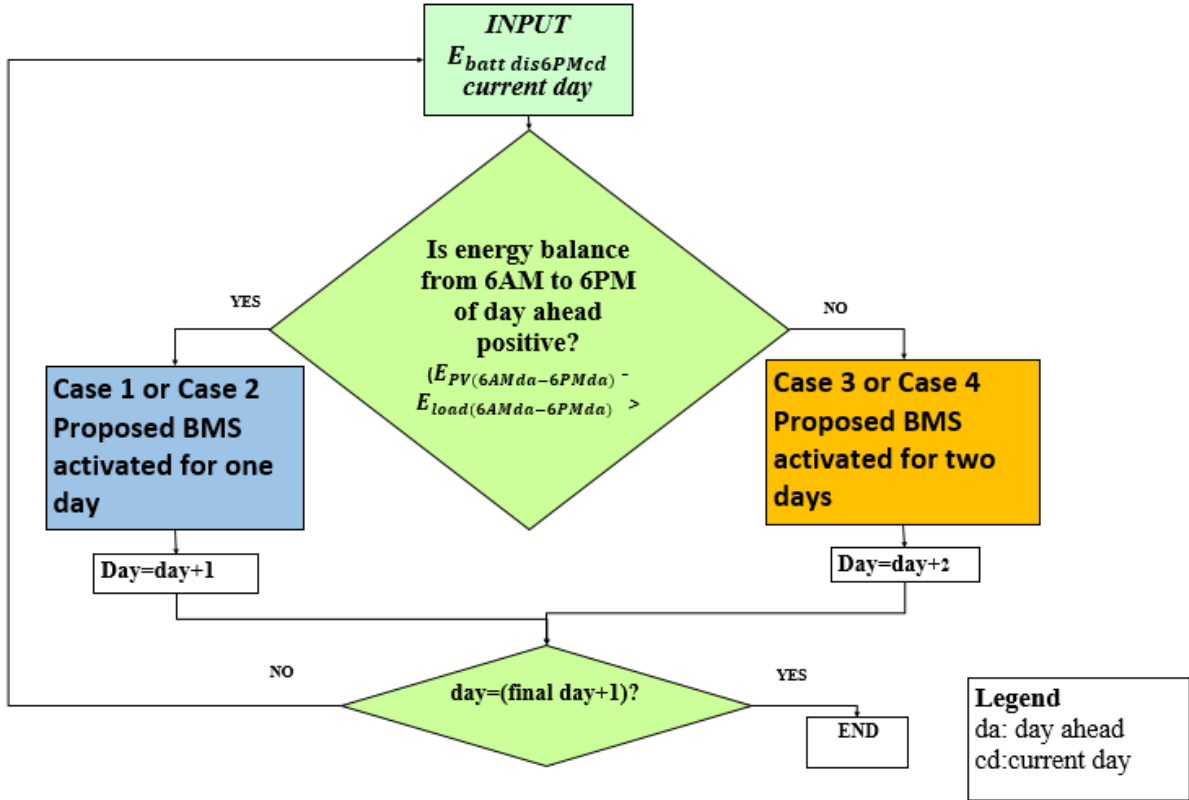


Figure 3.5.1: Proposed Battery Management System
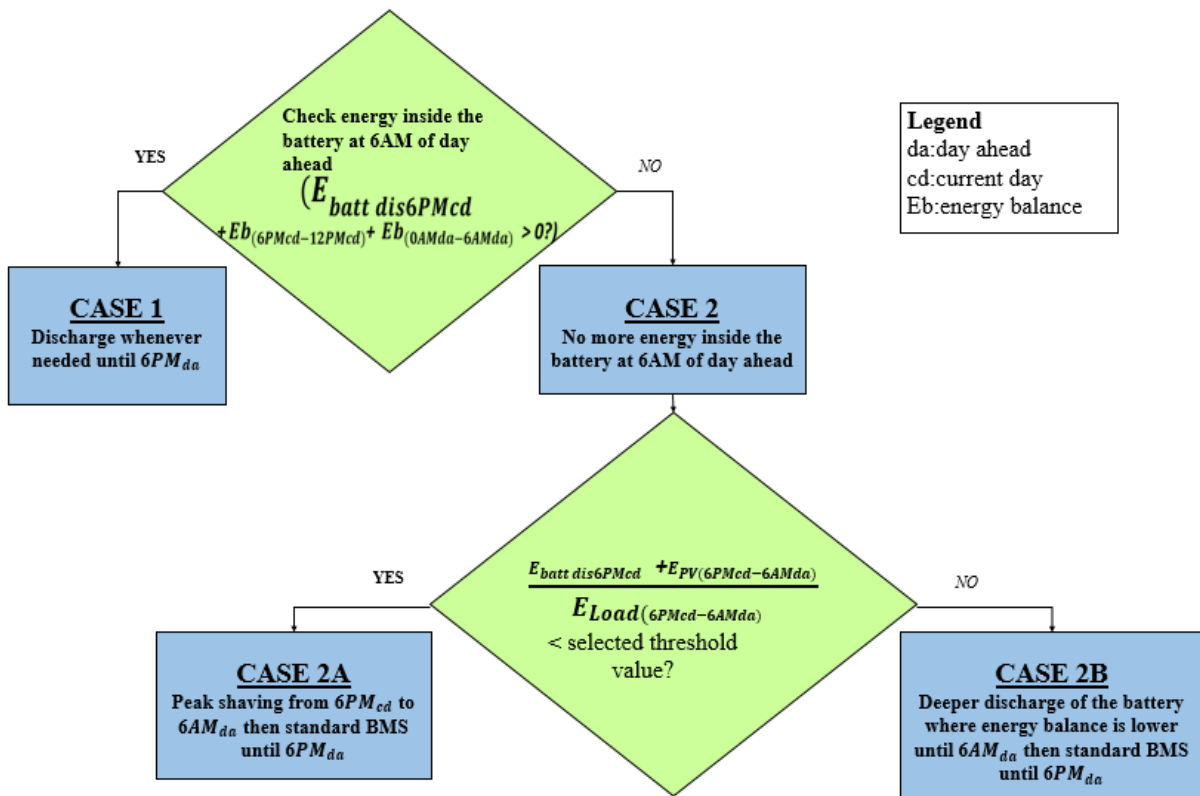
Figure 3.5.2: Proposed Battery Management System – CASE1 and CASE2
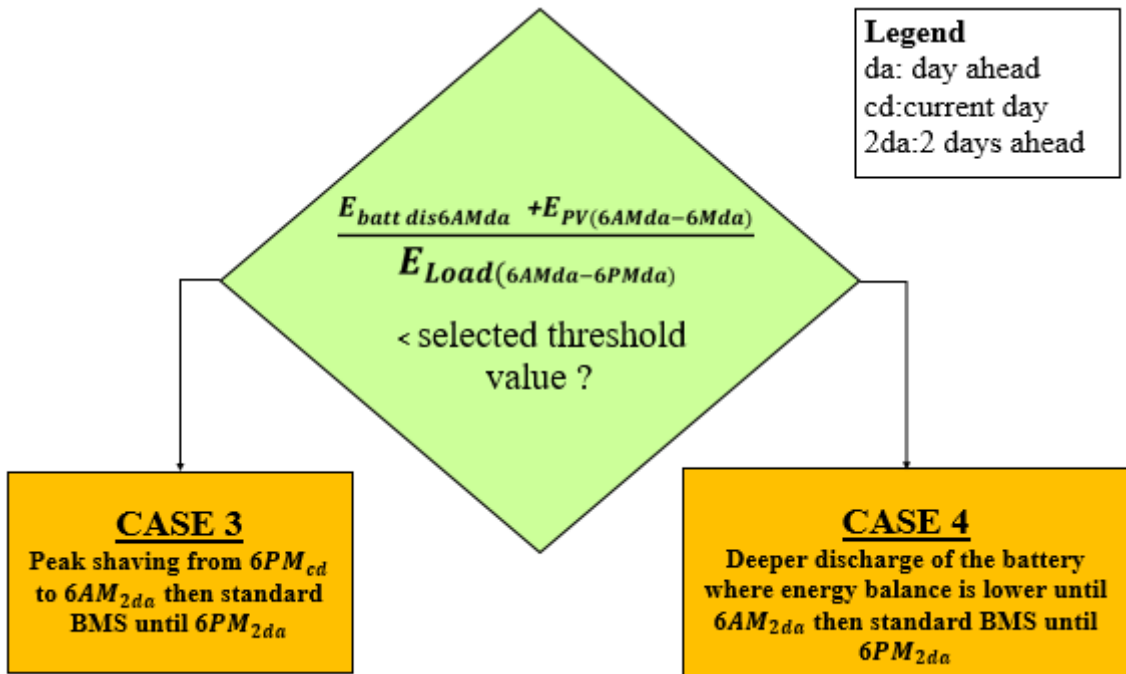
Figure 3.5.3: Proposed Battery Management System – CASE3 and CASE4

The proposed BMS receives as inputs the energy inside the battery available for discharge at 6PM of the current day and the current day itself. The first input $E_{battdis6PMcd}$ $[kWh]$ can be calculated as:

$$E_{battdis6PM_{cd}} = (SOC(6PM_{cd}) - 0.2)C_{batt} \qquad (3\text{-}12)$$
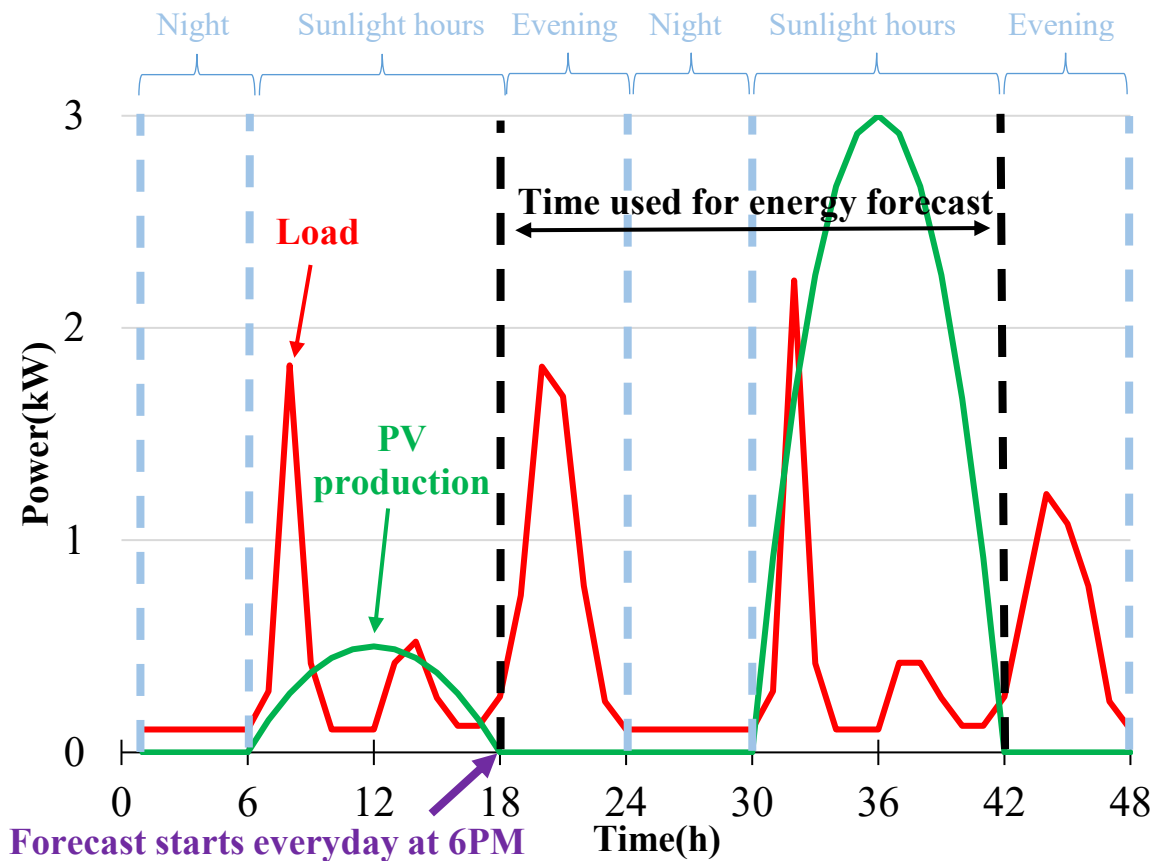

Figure 3.6: Proposed BMS with starting time and one day forecast

Once identified the two inputs, it is necessary to understand if the energy balance from 6AM to 6PM of the day ahead is positive and if the battery still contains some energy available for discharge at 6AM of the next day. Four possible cases can be distinguished:

Case 1

This is the best case since the energy balance from 6AM to 6PM of the next day is positive and the battery has still some energy available for discharge at 6AM of the next day. In this case, there is no limitation to SOC_{min} which will be equal to 0.2 for the entire period. It is then possible to discharge the battery every time that it is requested.

$$SOC_{\min(6PM_{cd}-6PM_{da})} = 0.2 \qquad (3\text{-}13)$$

Case 2

This is the case in which the energy balance from 6AM to 6PM of the next day is positive but the battery cannot be discharged any more at 6AM of the next day.
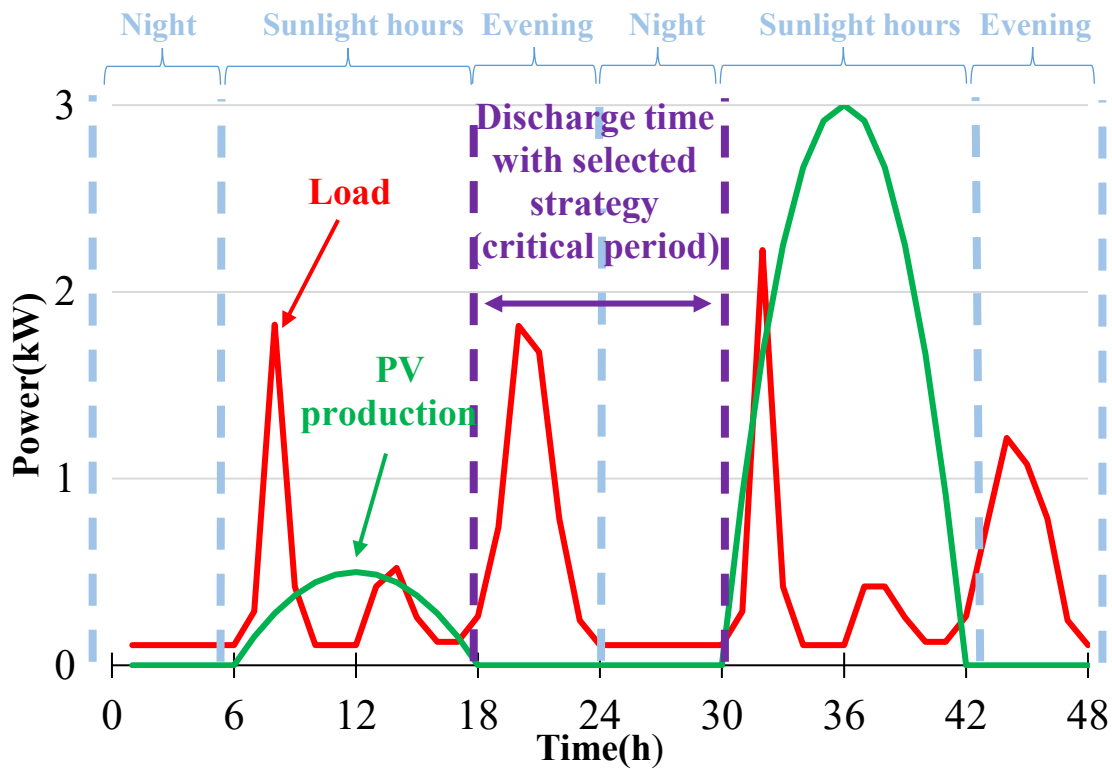

Figure 3.7: Critical period for case 2

In this case, the proposed BMS checks the following ratio:

$$\frac{E_{battdis6PM_{cd}} + E_{PV(6PM_{cd}-6AM_{da})}}{E_{Load(6PM_{cd}-6AM_{da})}}$$

(3-14)

If this ratio is lower than a selected threshold value, the battery will be only used to face the peaks in the load from 6PM of the current day to 6AM of the next day then the Standard BMS will be used until 6PM of the next day (case 2A). Thanks to Peak Shaving, it is possible to reduce considerably the maximum power absorbed from the grid. Instead, if the previous ratio is higher than a selected threshold value, the battery will distribute its residual energy at 6PM of the current day in the two following time slots using Peak Shaving only when necessary (case 2B). In this last case, the battery will have to provide more energy when the energy balance is lower or more critical and less energy in time slots characterized by a higher energy balance buying energy from the grid when the SOC goes below the SOC_{min} of the corresponding time slot. The SOC_{min} in the time slots 6PM-12PM of current day and 0AM-6PM of the day ahead will be selected as follows:

$$SOC_{\min(6PM_{cd}-12PM_{cd})} = \frac{(C_{batt}0.2 + E_{battdis6PM_{cd}} - \frac{Eb_{(6PM_{cd}-12PM_{cd})}E_{battdis6PM_{cd}}}{Eb_{(6PM_{cd}-12PM_{cd})}+Eb_{(0AM_{da}-6AM_{da})}})}{C_{batt}}$$

(3-15)

$$SOC_{\min(0AM_{da}-6PM_{da})} = 0.2$$

(3-16)

Case 3

In case 3, the energy balance from 6AM to 6PM of day ahead is negative and the ratio between the energy provided to the load from 6AM to 6PM of day ahead (by PV and battery) and the forecasted load itself is lower than a selected threshold.

This means that the battery will be only used to face the peaks in the load from 6PM of the current day to 6AM of two days ahead using the Standard BMS in the last time slot.
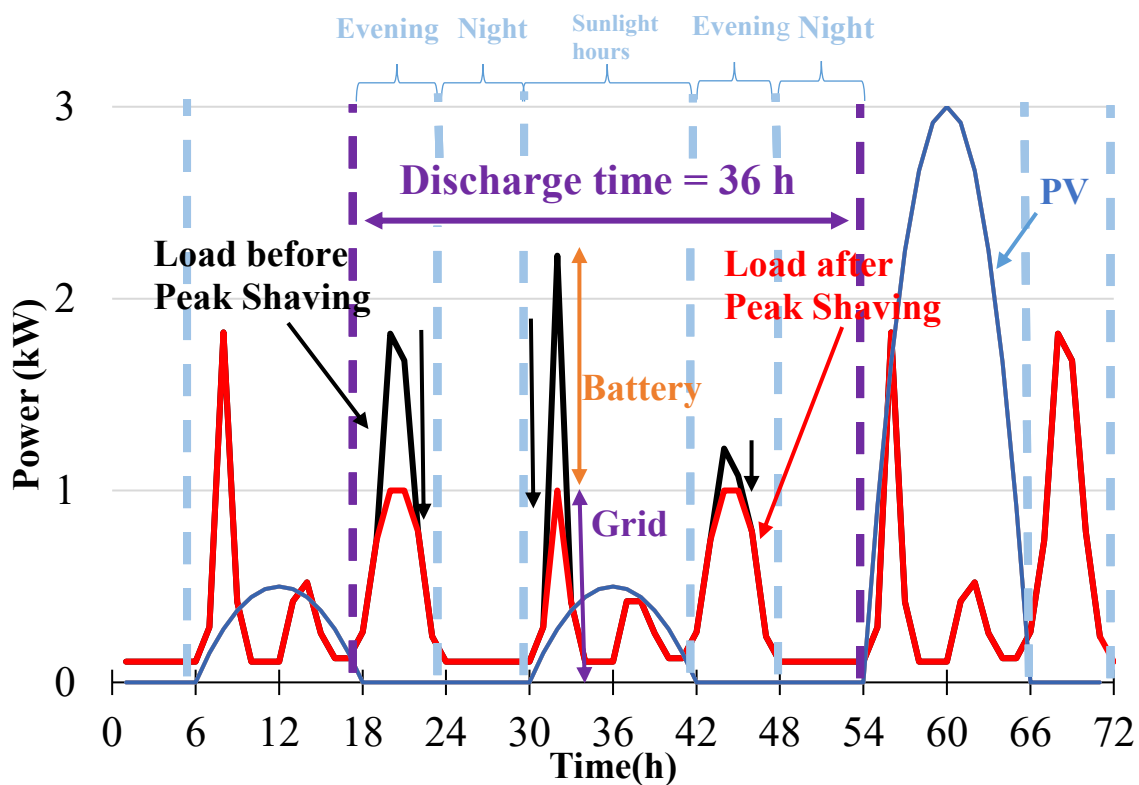

Figure 3.8: Example of Peak Shaving

Since the previous ratio is lower than a selected threshold, it would not be convenient to privilege self-consumption in the two days. Instead by using only Peak Shaving, it is possible to mitigate the peaks in the load limiting the use of the grid when consumption arises.

Case 4

In the last case, the energy balance from 6AM to 6PM of day ahead is negative and the ratio between the energy provided to the load from 6AM to 6PM of day ahead (by PV and battery) and the forecasted load itself is higher than a selected threshold.

This means that the residual energy inside the battery at 6PM of the current day will be distributed in five time slots using Peak Shaving when load exceeds a certain value.

The more the energy balance in the selected period is negative, the more energy will be provided by the battery.

Obviously, the amount of energy provided from the battery in the several time slots will tend to be lower with respect to the case 2B because the amount of energy inside the battery at 6PM of the current day has to be shared in more time slots. The SOC_{min} corresponding to the various periods will be summarized below:

$$SOC_{\min(6PMcd-12PMcd)} =$$

$$\frac{(C_{batt}0.2 + E_{battdis6PM_{cd}} - \frac{Eb_{(6PM_{cd}-12PM_{cd})}E_{battdis6PM_{cd}}}{sum(Eb_{(6PM_{cd}-6AM_{2da})})})}{C_{batt}} \qquad (3\text{-}17)$$

$$SOC_{\min(0AMda-6AMda)} =$$

$$\frac{(C_{batt}0.2 + E_{battdis6PM_{cd}} - \frac{(Eb_{(6PMcd-12PMcd)} + Eb_{(0AMda-6AMda)})E_{battdis6PM_{cd}}}{sum(Eb_{(6PM_{cd}-6AM_{2da})})})}{C_{batt}} \qquad (3\text{-}18)$$

$$SOC_{\min(6AMda-6PMda)} =$$

$$\frac{(C_{batt}0.2 + E_{battdis6PMcd} - \frac{(Eb_{(6PMcd-12PMcd)} + Eb_{(0AMda-6AMda)} + Eb_{(6AMda-6PMda)})E_{battdis6PMcd}}{sum(Eb_{(6PM_{cd}-6AM_{2da})})})}{C_{batt}} \qquad (3\text{-}19)$$

$$SOC_{\min(6PMda-12PMda)}$$

$$= \frac{\left(C_{batt}0.2 + E_{battdis6PMcd} - \frac{(Eb_{(6PMcd-12PMcd)} + Eb_{(0AMda-6AMda)} + Eb_{(6AMda-6PMda)} + Eb_{(6PMda-12PMda)})E_{battdis6PMcd}}{sum(Eb_{(6PM_{cd}-6AM_{2da})})}\right)}{C_{batt}}$$

$$(3\text{-}20)$$

$$SOC_{\min(0AM_{2da}-6PM_{2da})} = 0.2 \qquad (3\text{-}21)$$

CHAPTER 4: FEASIBILITY STUDY OF THE PROPOSED BMS - APPLICATION TO A RESIDENTIAL PV SYSTEM COUPLED WITH BATTERY STORAGE

The investigated PV system is a residential one and located in the North of Italy more precisely near Turin. The rated power of the single module is 235 Wp. All the PV modules have a tilt angle of 15° according to the inclination of the roof and are west oriented with an azimuth angle of 92°. The modules are made of polycrystalline silicon and are installed on a specific structure to guarantee a correct anchoring and a suitable ventilation. Another important characteristic of the modules is their size since it affects the amount of energy production. The size of the modules is the standard one which corresponds to 1640x992 mm.

Figure 4.1: Polycrystalline PV modules installed on a household roof

The characteristic of the modules can be summarized in the table 4.1:

Parameters	Values
Maximum Power (Pmax)	235W
Maximum power voltage (Vmp)	29.8V
Maximum power current (Imp)	7.89 A
Short circuit current (Isc)	8.29 A
Open circuit voltage (Voc)	37.6V
Module efficiency	14.44%
Maximum voltage (Usys)	DC1000V(TUV)
Power tolerance	0-3%
Fuses in series (Ir)	15°
Dimensions	Length=1640mm; Width= 992mm; Height= 40mm;
Solar cell	60 solar cells (156mm x 156mm) in connection arrays of 6 x 10 cells
Nominal operating cell temperature (NOCT) :	47 ± 2°C
Temperature coefficient of Pmax :	-0.44%/°C
Temperature coefficient of VOC :	-0.34%/°C
Temperature coefficient of ISC :	0.06%/°C

Table 4.1: Technical data of modules in Standard Test Conditions (G=1000 W/m^2, T=25°C, AM=1.5)

The adopted inverter is able to convert direct current into alternate current using the Pulse Width Modulation (PWM) technique. It can work in automatic way and it is provided of a MPPT to find the maximum power point of the PV generator at every instant.

The inverter is placed in the basement to avoid an increase in the dispersion current towards the ground due to excessive humidity, especially on rainy days. Another advantage of the inverter

location is the cooler and dryer air which allows the inverter to operate at higher efficiency. Other characteristics are: the double input section able to process two different arrays with independent MPPT logics, high speed MPPT algorithm, the transformer less configuration with an efficiency until 96.8% and finally the wide range of input voltages.

The inverter technical characteristics are summarized in the table 4.2:

Parameters	Values
Maximum DC input voltage (Vmax,abs)	600 V
DC activation input voltage(Vstart)	200 V (adj. 120...350 V)
Operating range DC input voltage (Vdcmin...Vdcmax)	0.7 x Vstart...580 V
Input DC nominal voltage(Vdcr)	360 V
Number of independent MPPT	2
DC connection	Connector PV Tool Free WM / MC4
AC grid connection	Monophase
AC nominal output voltage (Vac,r)	230 V
AC output voltage range	180...264 V
Maximum AC output current (Iac,max)	17.2 A
Contribute to short circuit current	19.0 A
Output nominal frequency (fr)	50 Hz / 60 Hz
Range output frequencies (fmin...fmax)	47...53 Hz / 57…63 Hz
Maximum efficiency (ηmax)	96.8%
Weighted efficiency (EURO/CEC)	96.0% / -

Table 4.2: Technical data of the inverter

As regards the battery, the technology adopted is lithium ion because it is the one which provides the highest depth of discharge. Its size has to be determined in order to minimize the maximum power absorbed from the grid without neglecting self-consumption. Another issue is the cost reduction related to this electrochemical device. This is possible by implementing a correct energy management which takes into account weather conditions and forecasted energy balance to understand when it is better to discharge the battery. Capacities chosen for the simulations range between 1kWh and 5kWh since these sizes are the ones typically used in residential storage systems. The technical specification of the single battery element are listed in the table 4.3.

Parameters	Values
Battery rated capacity	250 Ah
Battery rated voltage	40 V
Lifetime	10 years (3500 cycles at DoD=80%)
Maximum power	2kW to 10kW
Charging efficiency	0.88

Table 4.3: Technical data of single battery module

Figure 4.2: Residential battery module

The architecture of the system with all the involved components, the DC and AC buses together with all the possible power flows is illustrated in the figure 4.3.
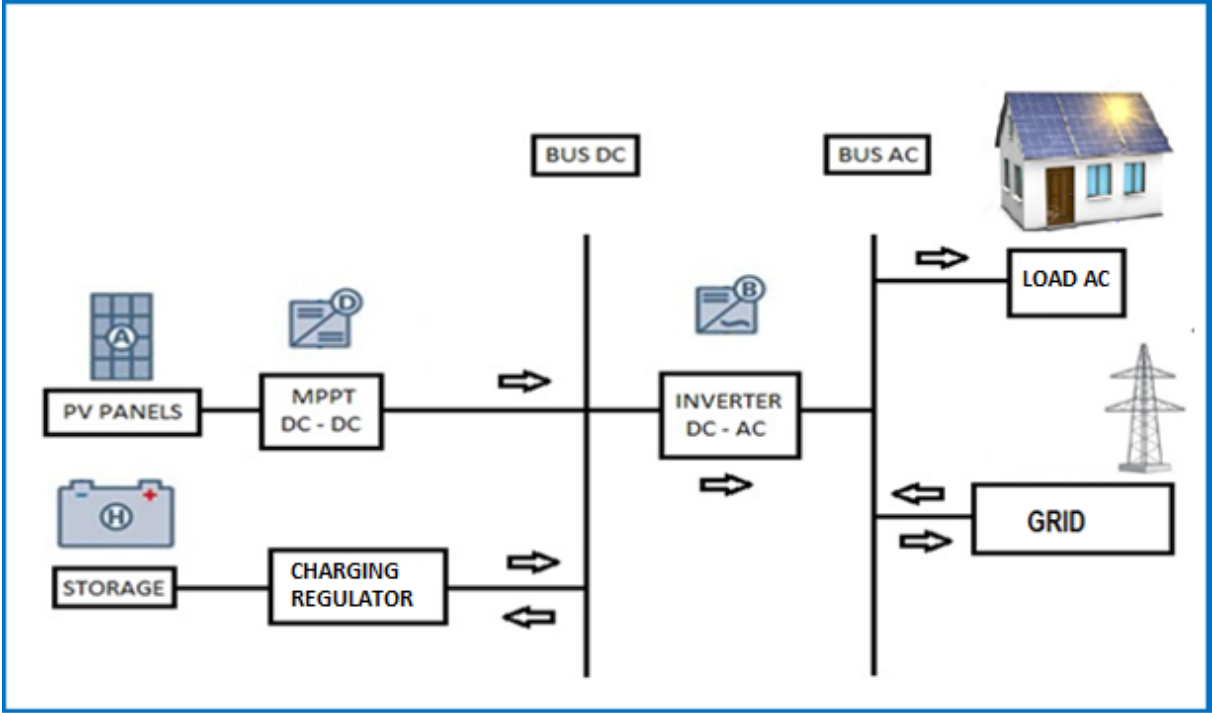

Figure 4.3: System Architecture

4.1 DEFINITION OF THE HOUSEHOLD LOAD

In order to define correctly the management of the battery, it is important to highlight the characteristics of the household load. Typically, most of the contribution to the electrical consumption is due to air conditioners especially on summer time.

Other important loads are water heater systems, refrigerators and household appliances such as ovens and washing machines but also PCs and televisions.
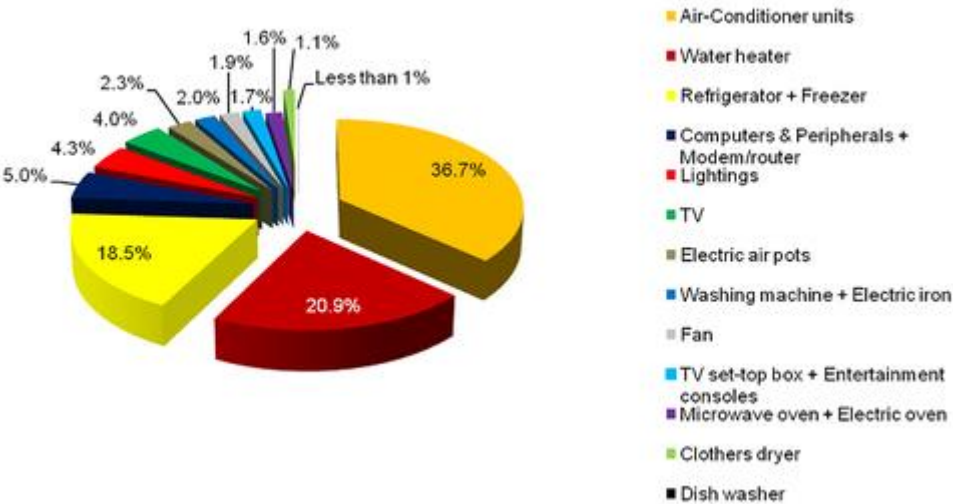

Figure 4.4: Average household electrical consumption

Generally, the electrical consumption has two peaks; one in the early morning and the other one in the evening between 19 o'clock and 22 o'clock. One of the main purposes of storage systems is to face these peaks reducing the grid intervention and so the cost of the bill. The annual electrical consumptions range between 3000 kWh and 3500 kWh according to the number of members of the house and on their lifestyle. This is to take into account when sizing a PV plant connected to the grid. It is possible to state that the electric consumption is slightly higher in summer due to the functioning of the air conditioners whereas in winter it is slightly lower because of the lower consumption of water heaters. Lightings does not account a lot in the

global consumption but it is sure that on winter they are on for longer with respect to summer time.

4.2 NOTES ON MONTHLY IRRADIATION IN TURIN

One aspect to take under consideration when dealing with the design of a PV plant is the irradiation of the place in which it will be installed. Thanks to the data about solar irradiation, it is possible to understand when the PV power output will be higher and when it will be lower. As expected, solar production will tend to increase during summer months and decrease during winter months. Another important aspect that one has to take into account is the optimal inclination of PV panels. The optimal inclination will be higher in winter months since the sun is low at the horizon and lower in summer months because, in that period, the sun is high at the horizon. The best inclination is a trade-off which aims not to penalize PV production both on summer and on winter. Since the chosen location is Turin and the inclination of PV modules is 15°, data about monthly solar irradiation with the selected inputs will be illustrated in the table 4.4.

Month	H_{opt}	$H(15)$	I_{opt}
Jan	2730	2070	66
Feb	4050	3250	60
Mar	5260	4660	47
Apr	5320	5180	31
May	5850	6090	18
Jun	6170	6620	12
Jul	6630	7030	15
Aug	6210	6200	27
Sep	5420	4960	42
Oct	3810	3250	53
Nov	2750	2150	63
Dec	2540	1880	68
Year	4730	4450	38

H_{opt}: Irradiation on optimally inclined plane (Wh/m^2/day)
$H(15)$: Irradiation on plane at angle: 15deg. (Wh/m^2/day)
I_{opt}: Optimal inclination (deg.)

Table 4.4: Typical daily irradiation at an inclination of 15° and at optimal angle for every month of the year

Figure 4.5: Yearly sum of global irradiation at optimal angle in the selected area

The figure 4.5 shows the yearly sum of global irradiation at optimal inclination in the North West of Italy and also in Turin. As it is possible to see, in the selected city, this value is about 1800 kWh/m^2. Obviously the largest contribution to this value comes from the irradiation in the summer months in which the peaks of the irradiation are reached.

4.3 SELECTION OF THE SUITABLE PERIOD FOR SIMULATIONS

In order to appreciate better the effectiveness of the proposed BMS, the simulations should be performed in months characterized by great variability and low solar radiation such as winter months because on summer there is usually a PV over production and so there is no need to check continuously the amount of energy that the battery can provide to the load. The best period to make the simulations is the month of December since this month is characterized by the alternation of sunny days and cloudy days and it is the most critical for what concerns the peaks of power absorbed from the grid. Besides the PV power output is limited and so, in days with a large amount of power consumed by the load, the energy balance will tend to be negative. This will cause a more rational use of energy inside the battery in the previous day to avoid the discharging in a too short time. The behaviour of PV power output and of the load during four days on December is shown in the figure 4.6.
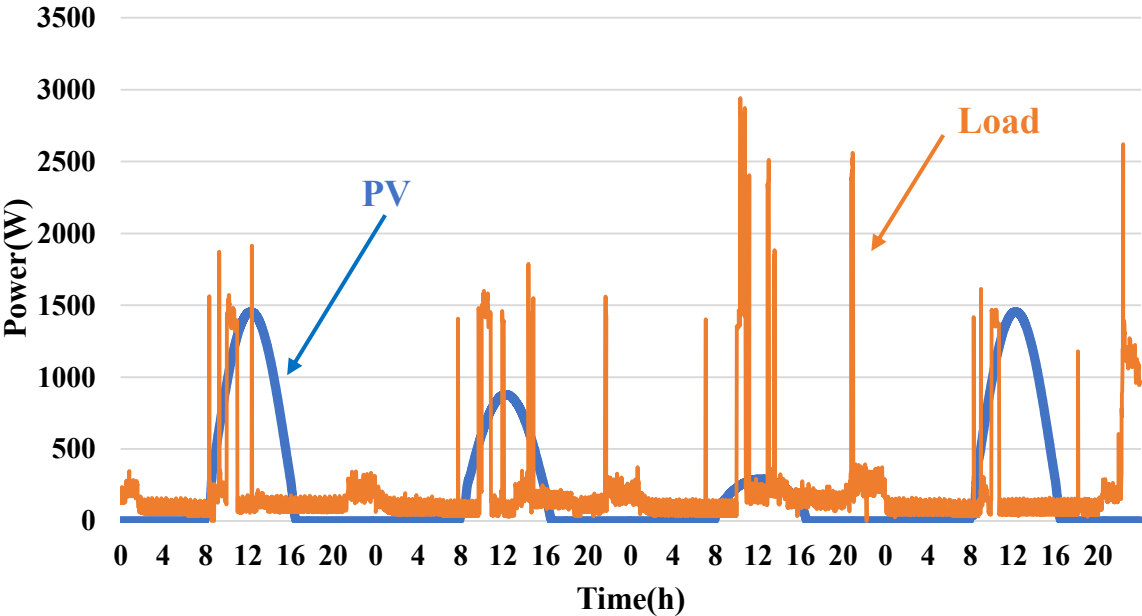

Figure 4.6: Behaviour of PV power output and load during four days on December

As it is possible to see, during these days, the PV output power, referred to a nominal power of 3kWp, is quite low whereas the load is characterized by the presence of peaks which can be reduced thanks to the use of a storage system. By looking at the graph, the period of PV production lasts about 8 hours a day that is generally from 8AM to 4PM. Obviously during evening and night the PV power output is null and so the battery will have to face the load in that period.

4.4 SIZING PROCEDURE: INPUT DATA

The input data which are used to find the configuration that minimizes the maximum power absorbed from the grid in the selected month are: The peak power of the PV plant P_{PV}, the capacity of the battery C_{Ebatt}, the maximum value of the load after the adoption of Peak Shaving $P_{maxload}$ and finally the *Threshold value* which decides between Peak Shaving or sharing of battery energy content in more time slots. The values which can be assigned to these input data can be summarized in the table 4.5.

$P_{PV}(kW_p)$	2	3	4	5	6
$C_{Ebatt}(kWh)$	1	2	3	4	5
$P_{maxload}$ *with Peak Shaving*(kW)	0.5	1	1.5	2	
Threshold value (for cases 2,3,4) (%)	50	60	70	80	

Table 4.5: Input data for simulations

The maximum power that the battery can release or absorb is supposed to be twice its capacity. There are 400 possible combinations, each one is simulated with the proposed BMS thanks to the software Matlab® which will give the outputs of interest.

4.5 EXAMPLE OF SIMULATIONS

Battery discharge whenever needed

In this case, there is no limitation on the minimum state of charge which remains equal to 0.2 until 6PM of the day ahead. This happens when the energy balance from 6AM to 6PM of the next day is positive and the battery still contains some energy at 6AM of day ahead. There are no differences between the Standard BMS and the proposed BMS in this situation. The figure 4.7 shows the behaviour of PV, load, battery and grid in such case from 0AM of 9/12 to 6PM of 10/12 according to the User Convention meaning that power absorbed from battery and grid is positive whereas power released is negative.
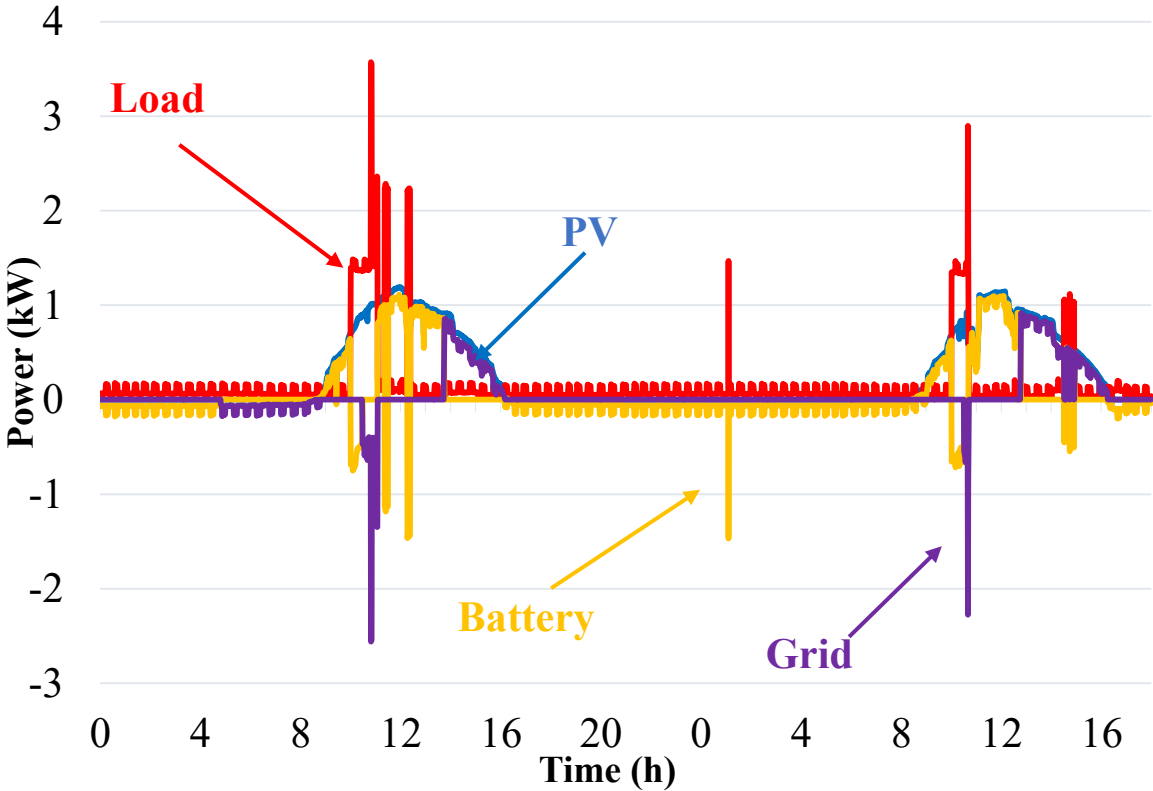

Figure 4.7: Simulation of the proposed and standard BMS from 0AM of 9/12 to 6PM of 10/12.

Another important thing to show is the behaviour of the battery state of charge (SOC) during the entire period. The graph in figure 4.8 shows that the SOC is limited between 0.2 and 1 and that this quantity goes up and down if the battery accumulates or release power. It is possible to see that both in day 9/12 and in day 10/12, the largest amount of charge is stored by the battery from around 12AM to 2PM. In the two days, the SOC, starting from its minimum value at around 12AM, is able to reach its maximum value at the end of the charging process. This allows the battery to release a large amount of power during evening and night.
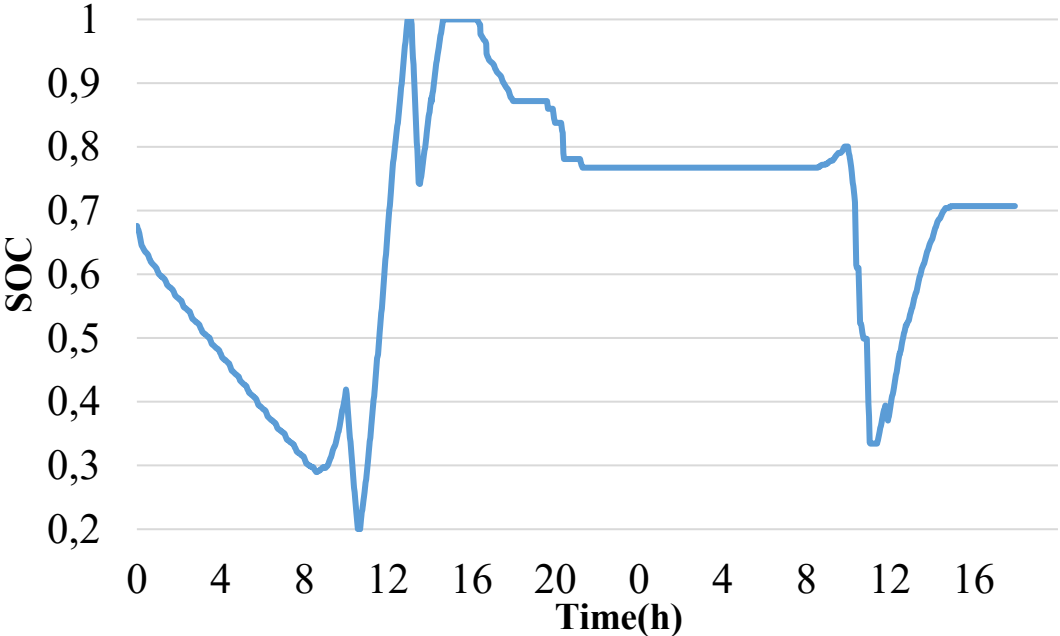

Figure 4.8: Behaviour of battery SOC during the considered days for Modified and Standard BMS from 0AM 9/12 to 6PM 10/12

Peak Shaving

The technique of Peak Shaving is activated in case of criticality that is when the ratio between the forecasted renewable energy provided to the load and the load itself goes below a certain threshold which will be varied during simulations.

Thanks to Peak Shaving, it is possible to face the peaks in the load thus reducing the use of the grid when consumption increases. With the use of Peak Shaving, it is possible to minimize the maximum power exchanged with the grid during the selected month thus reducing the contract power. Peak Shaving also creates a benefits for the grid since it can provide to the load a more constant power profile thus reducing unbalances in power distribution. When using Peak Shaving, it is important to find a trade off in the maximum value of the load over which the battery intervenes; if this value is too high self-consumption risks to be excessively penalized whereas if this value is too low the battery could discharge too fast without being able to face all the peaks which may occur.

The graph in figure 4.9 shows that the proposed BMS is able to cut the peaks that occur from 6PM of 15/12 to 6PM of 16/12 in a good way reducing the maximum power bought from the grid which does not exceed the value of 2kW. Peak shaving is particularly powerful when the load becomes very high, as from 10AM to 12AM of 16/12, avoiding possible peaks which could provoke stresses on the grid. Obviously, by using only the technique of Peak Shaving during the whole considered period, self-consumption turns out to be a little more penalized in the proposed BMS with respect to the Standard BMS with a difference of 0.89kWh.
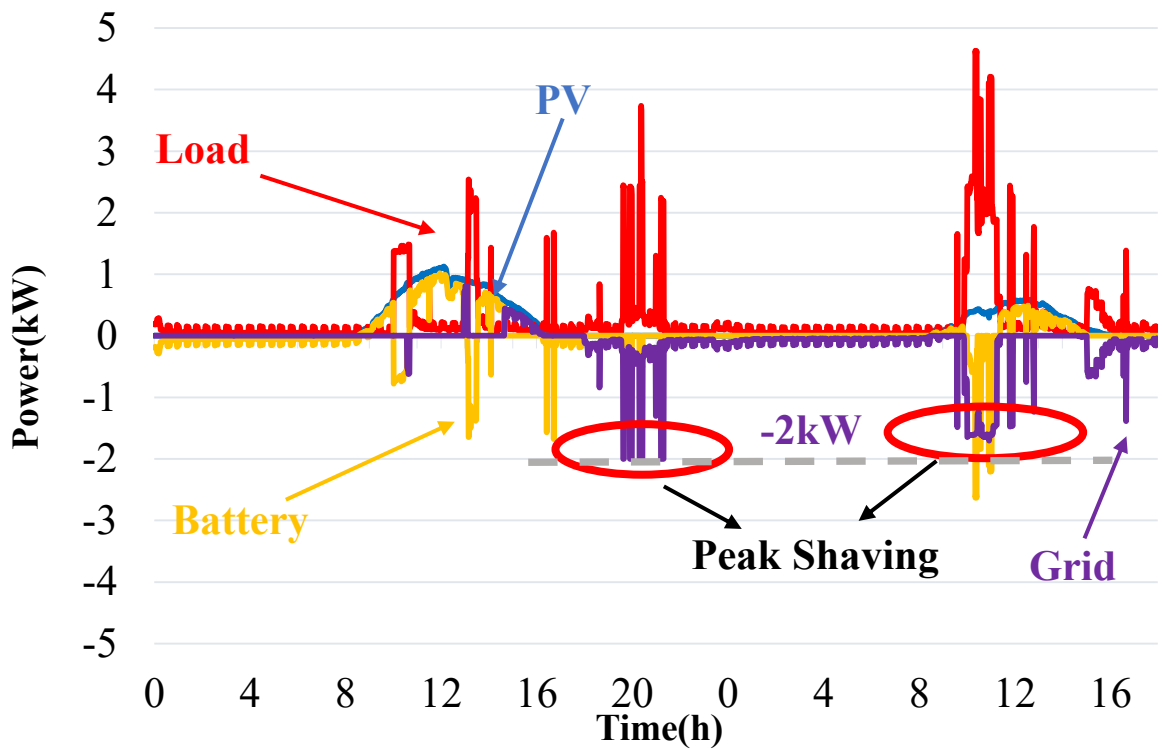
Figure 4.9: Simulation with proposed BMS from 0AM of 15/12 to 6PM of 16/12
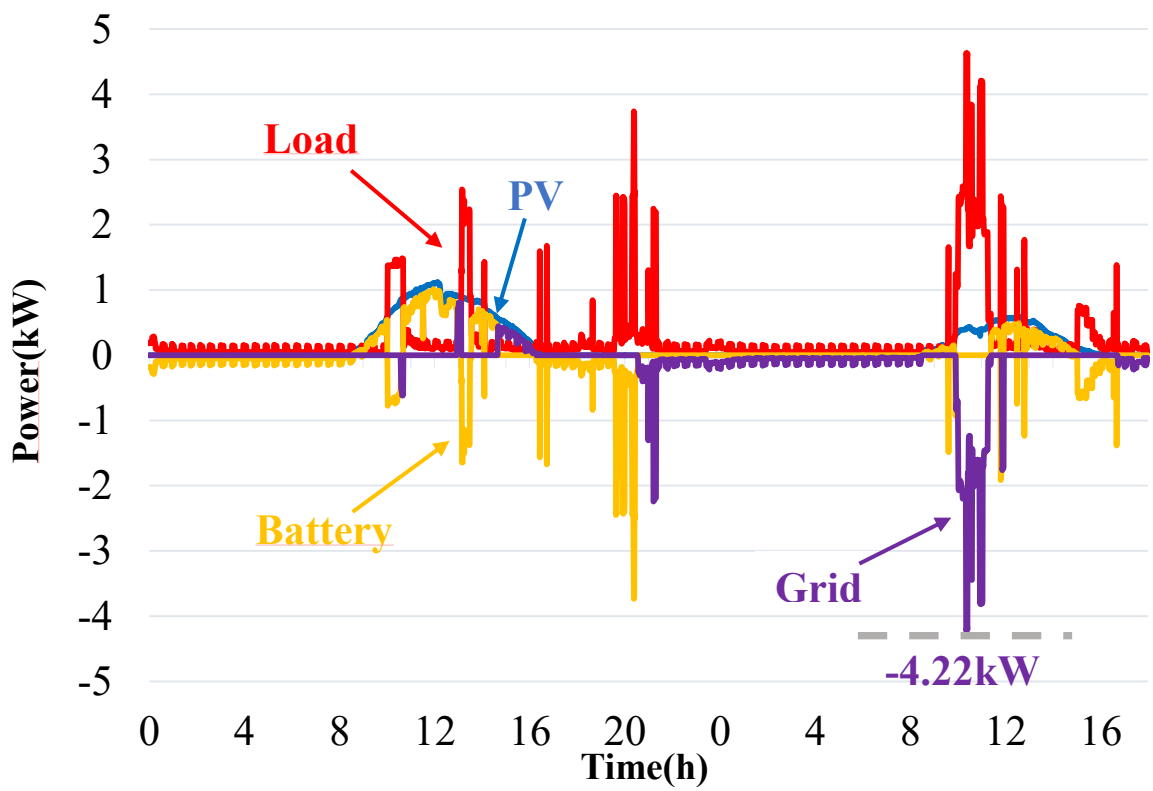
Figure 4.10: Simulation with Standard BMS from 0AM 15/12 to 6PM 16/12

As expected, even the SOC will be different using the proposed BMS with respect to the Standard BMS in the selected period. In the Standard BMS, the battery is only able to face the peak from 6PM to 8PM of 15/12 before its SOC reaches its minimum value. Instead, using the proposed BMS, the SOC, starting from 6PM of 15/12, will drop down only when the load exceeds a certain value avoiding the immediate discharge. In this way, a more rational use of the energy inside the battery is achieved such that the battery will be able to face even the other peak which occurs from around 10AM to 12AM of the 16/12.
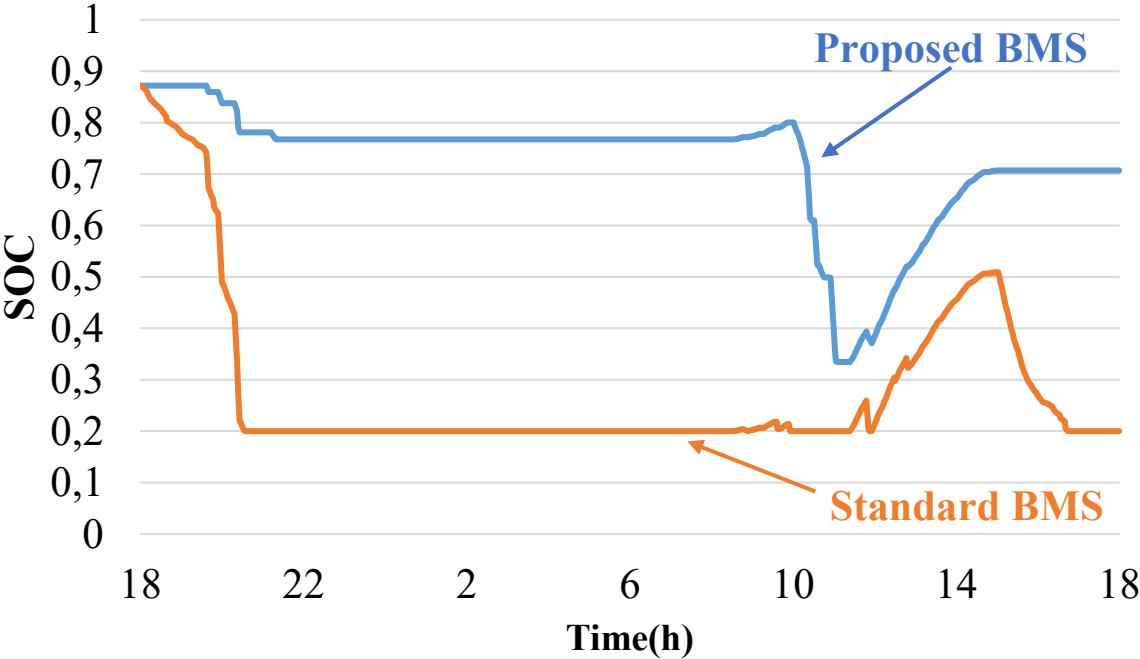

Figure 4.11: Behaviour of battery SOC for Proposed and Standard BMS from 6PM of 15/12 to 6PM of 16/12

Sharing of battery energy content in more time slots

Sharing of battery residual energy in more time slots is performed when the ratio between the forecasted renewable energy provided to the load and the load itself goes above a certain threshold. This allows to use the battery for more time slots even with low residual energy. When the load exceeds a certain threshold, Peak Shaving is activated and the battery will only intervene to face the peaks avoiding a too fast discharge.

The graph in Figure 4.12 shows the sharing of the residual energy content of the battery at 6PM of 2/12 in five time slots each one characterized by a selected SOC_{min}. As it is possible to see, the battery will provide the largest amount of its energy (1.34kWh) from 6AM to 6PM of 3/12 since the energy balance in that time slot is the lowest between the considered ones (-3.3 kWh) due to the use of an electric boiler. The lowest amount of energy (0.2kWh) is provided by the battery in the time slot which goes from 0AM to 6AM of 4/12 in which consumption is nearly negligible. When the load exceeds 1.5 kW, Peak Shaving is performed thus limiting the use of the battery with the aim to minimize the maximum power bought from the grid. This occurs from 10AM to 12AM and from 8PM to 9PM of 3/12. As one can see, with the proposed BMS the maximum power absorbed from the grid during the considered period is a little more than 2kW whereas using the Standard BMS it is nearly 3kW.
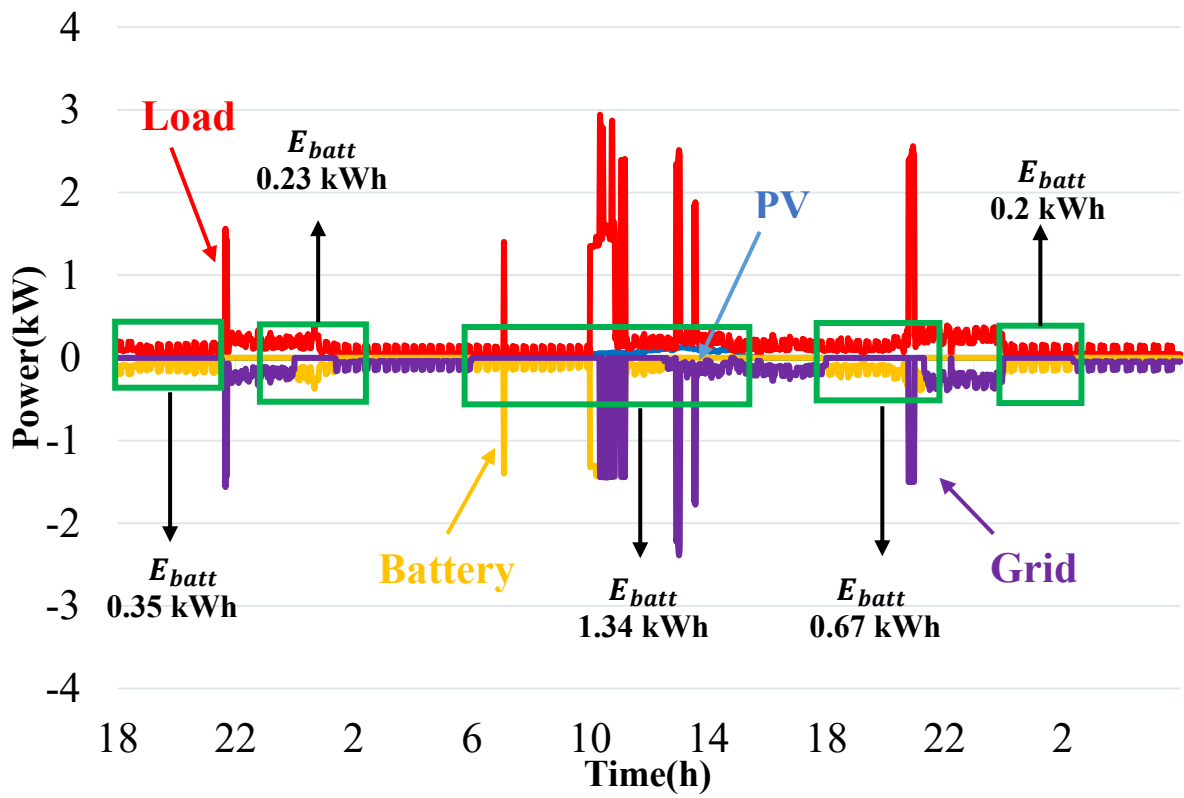
Figure 4.12: Simulation with proposed BMS from 6PM of 2/12 to 6AM of 4/12
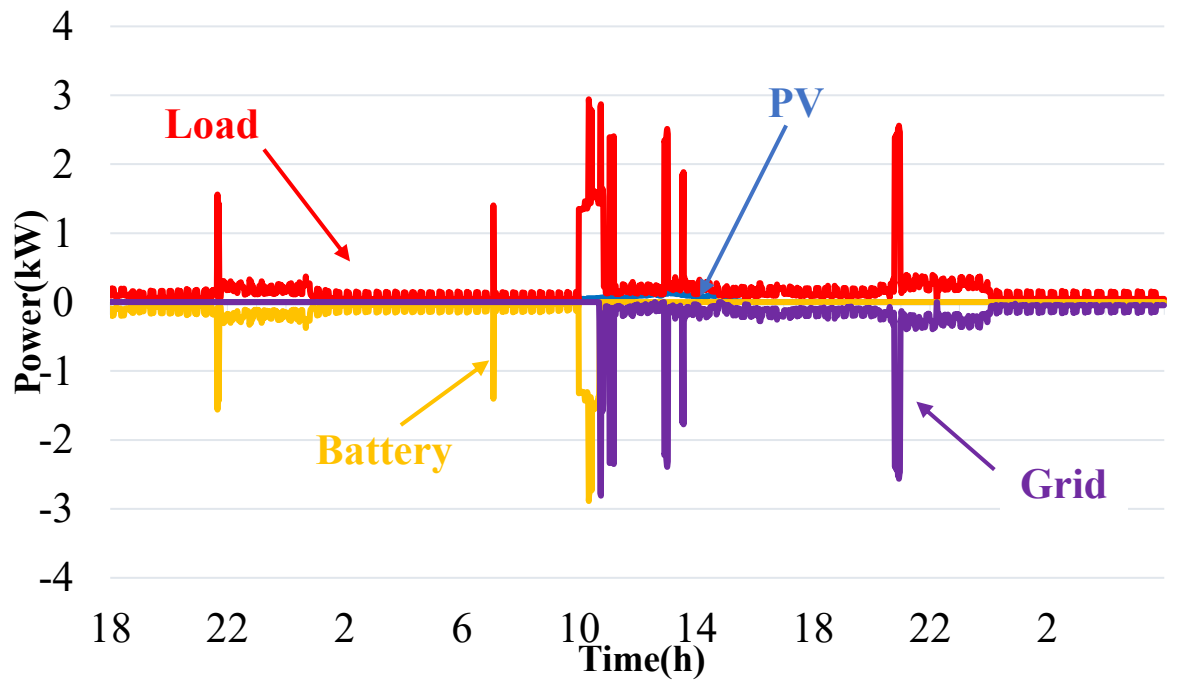
Figure 4.13: Simulation with Standard BMS from 6PM of 2/12 to 6AM of 4/12

91

In the figure 4.14, it is possible to see the difference between the SOC in the two BMS. Considering the proposed BMS, the values of SOC_{min} in the five time slots are:

- 0.75 from 6PM to 12PM of 2/12

- 0.7 from 0AM to 6AM of 3/12

- 0.4 from 6AM to 12AM of 3/12

- 0.25 from 6PM to 12PM of 3/12

- 0.2 from 0AM to 6AM of 4/12
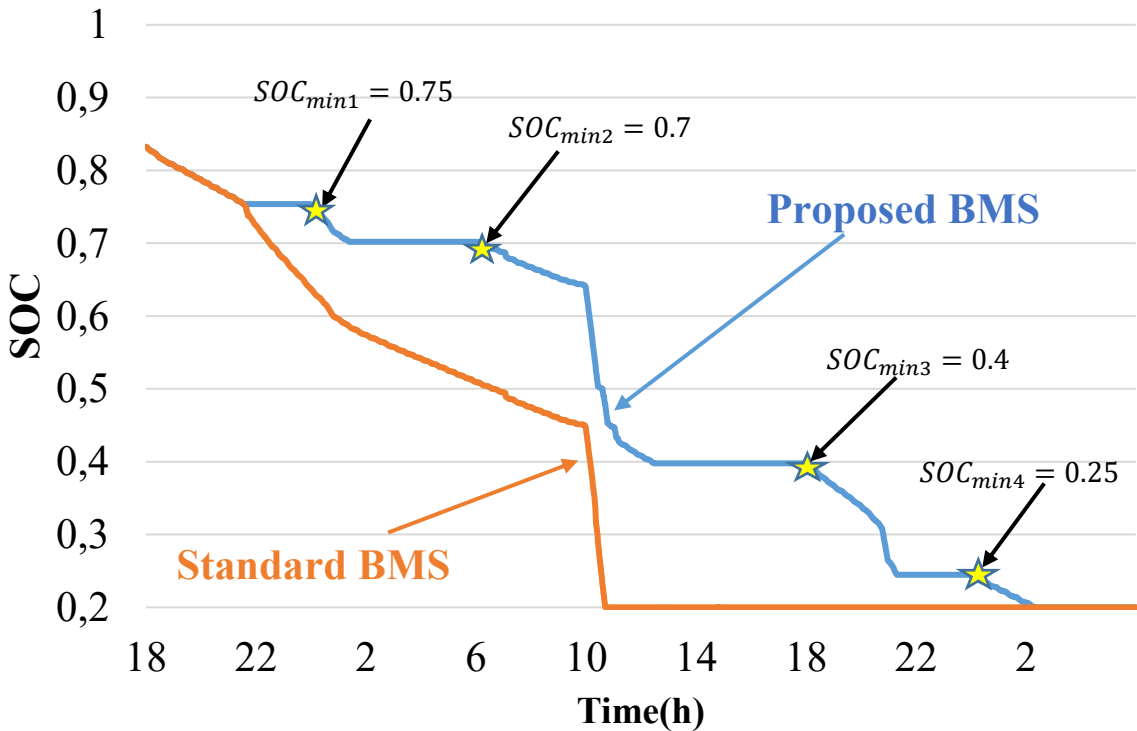
Figure 4.14: Behaviour of SOC for Proposed and Standard BMS from 6PM of 2/12 to 6AM of 4/12

4.5 SIZING PROCEDURE: OUTPUT

Using the proposed BMS, a large number of simulations have been performed with the inputs in the table 4.5. The best combination in order to reduce the maximum power absorbed from the grid has turned out to be the one in the table 4.6.

$P_{PV}(kW_p)$	4
$C_{Ebatt}(kWh)$	2
$P_{maxload}$ *with Peak Shaving*(kW)	2
Threshold value (for cases 2,3,4) (%)	50

Table 4.6: Selected configuration - OUTPUT

As it is possible to see, 18 modules with a power of 235Wp each will be necessary to reach the peak power of the PV plant equal to 4kWp. The selected size of the battery is quite small (2kWh) and this has a good impact on the investment cost. In case of Peak Shaving, the battery will intervene when the load exceeds 2kW satisfying the peaks. By looking at the table 4.7, the selected combination allows an improvement in the maximum power absorbed from the grid of about 40% which passes from 4.22kW to 2.56kW. The variation in self-consumption is negligible with a difference of just 4kWh with respect to the Standard BMS. Even the injection to the grid is nearly the same with the two BMS.
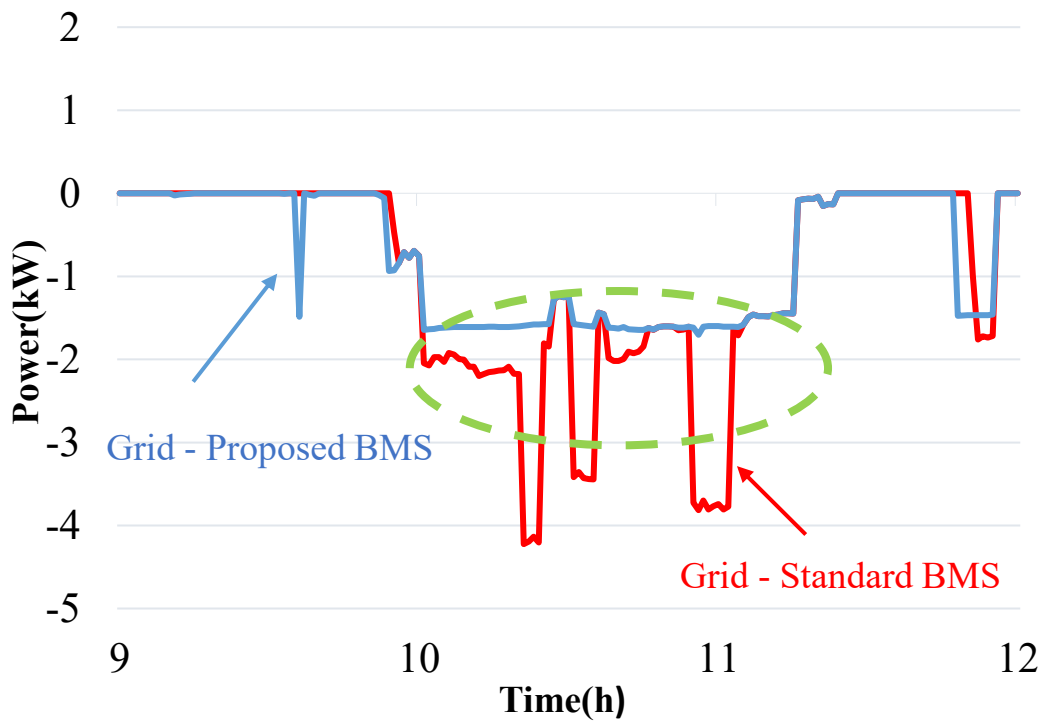
Figure 4.15: Improvement in maximum power absorbed from the grid with the proposed BMS from 9AM 16/12 to 12AM 16/12 related to Figures 4.9 and 4.10

Monthly Output	proposed BMS	standard BMS
Self-consumption(kWh)	43	47
Absorption from the grid(kWh)	30	28
Injection to the grid(kWh)	42	39
Self-sufficiency/load (%)	38	41
Self-consumption/PV production (%)	31	34
Maximum power absorbed from the grid(kW)	-2.56	-4.22
Maximum power injected to the grid(kW)	1.36	1.36

Table 4.7: results with selected configuration

The proposed BMS shows a higher number of minutes in which the power absorbed from the grid is between 0.5kW and 2kW. In all other ranges, the proposed BMS is preferable with respect to the standard BMS. The largest improvement is in the range 2 – 2.5 kW with a difference of 47 minutes between the two BMS. The histogram in figure 4.16 shows that, using the Standard BMS in the selected period, there are some minutes with powers absorbed from the grid showing peaks which range from 3kW to 4.5kW. Instead, making use of the proposed BMS, there are no minutes in which the maximum power absorbed from the grid exceeds 3kW thus making a good impact on contract power.
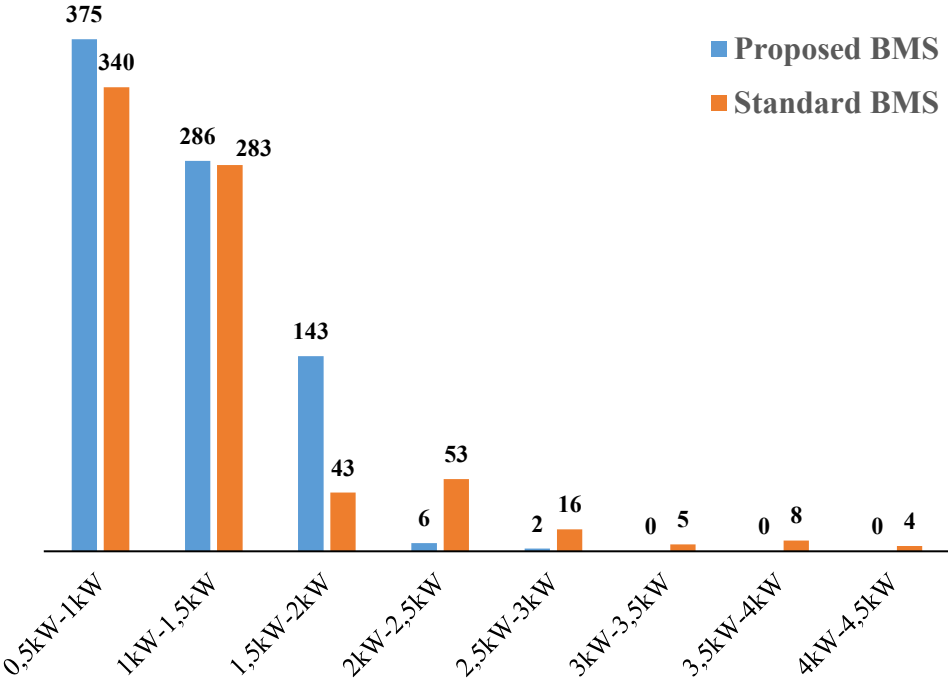

Figure 4.16: Number of minutes for ranges of power absorbed from the grid during December

There are some combinations which show some improvements, even if lower with respect to the selected one, in the maximum power absorbed from the grid. Even in these cases, self-consumption remains nearly the same with respect to the Standard BMS.

From the table 4.8, it is possible to notice that with a battery of 5kWh, that is the largest size according to the input parameters, the improvement is just of 8.8% which is far from the one obtained with the selected configuration. So, it is possible to state that the improvement in the maximum power absorbed from the grid is not proportional to the size of the battery.

$P_{PV}(kW_p)$	C_{Ebatt} (kWh)	$P_{maxload}$ with Peak Shaving(kW)	Threshold value (for cases 2,3,4) (%)	STD BMS Max. power absorbed from the grid(kW)	PROPOSED BMS Max. power absorbed from the grid(kW)	Improvement %
2	1	2	70	-4.42	-4.00	9.5
3	2	2	80	-4.33	-3.91	9.7
5	5	1	60	-4.10	-3.74	8.8

Table 4.8: other possible configurations.

Conclusions

The investigated BMS allows a great reduction in the maximum power absorbed from the grid, facing the peaks in the load which occur during the selected month. The maximum power absorbed from the grid is 2.56kW using the proposed BMS whereas it is 4.22kW with the Standard BMS obtaining an improvement of 40%. By reducing the peaks, the user has the possibility to reduce the contract power from 4.5kW to 3kW with consequent savings on grid services. The variation in self-consumption is negligible with respect to the standard BMS.

It is convenient to apply the modified BMS in months characterized by a certain variability without considering the ones where there is an over production of solar energy because otherwise there would be no need to check continuously the residual energy inside the battery.

The configuration which minimizes the maximum power absorbed from the grid is 4kWp of PV and 2kWh/4kW for the battery. This reduction is achieved with a relatively small battery with a consequent benefit on the investment cost. The maximum power over which the battery intervene in case of Peak Shaving has been selected equal to 2kW whereas the threshold value to decide between Peak Shaving or sharing of battery energy content is equal to 50%.

The first limit of the proposed BMS is the reliability of the energy balance forecasts which depend on weather forecasts and on an average household consumption. The reliability is then more related to the one of weather forecasts because the household consumption remains nearly the same. The second limit of the proposed BMS is related to the complexity of the inverter which has to be provided with an Internet connection which may make the cost of the system arise.

References

[1] https://it.wikipedia.org/wiki/Energia_solare

[2] enerMENA - Advanced CSP Teaching Materials - Chapter 2 - Solar Radiation,2016

[3] Appunti del prof. G. Fracastoro - corso "*Technology for renewable energy sources*" - Solar radiation, 2016

[4] Appunti del prof. G. Fracastoro - corso "*Technology for renewable energy sources*" - Solar angles, 2016

[5] F. Spertino, "*Conversione Fotovoltaica dell'Energia*", Dip. Ingegneria Elettrica, Politecnico di Torino, Dispensa 2010

[6] F. Spertino, Lezioni di "*Sistemi per la produzione dell'energia elettrica*" -Politecnico di Torino, Ed. 2013

[7] F. Spertino, R. Carelli, "*Impianti fotovoltaici di piccola taglia*", CLUT, 2008

[8] F. Spertino, A. Abete, "*Generatori e Impianti Fotovoltaici*", Dip. Ingegneria Elettrica, Politecnico di Torino, CELID, 2001

[9] F. Spertino, "*Guida all'integrazione architettonica delle installazioni solari negli edifici*", 2011

[10] Ciocia Alessandro, "*Sistema fotovoltaico ad alte prestazioni integrato in barriere acustiche*", Tesi di Laurea Specialistica, 2012

[11] Scaglia Fabio, "*Studio di fattibilità di un sistema con fotovoltaico, eolico e accumulo, integrato da gruppo elettrogeno, per stazione radio*", Tesi di Laurea magistrale, 2017

[12] Ciocia Alessandro, "*Optimal Power Sharing between Photovoltaic Generators, Wind Turbines, Storage and Grid to Feed Tertiary Sector Users*", 2017

[13] Nasim Jabalameli, "*Rooftop PV with Battery StorageFor Constant Output Power Production*",2013

[14] P. Breeze, "*Power Generation Technologies*", Second edition, Chapter 10 "Power System Energy Storage Technologies", Pages 195-221, Elsevier, 2014.

[15] RSE (Ricerca Sistema Energetico), "*L'accumulo di energia elettrica*", Il Melograno editore, 2011.

[16] D. Rand, P. Moseley, "*Electrochemical Energy Storage for Renewable Sources and Grid Balancing*", Chapter 13 "Energy Storage with Lead–Acid Batteries", Pages 201-222, Elsevier, 2015.

[17] M. Buonomo, "*Batterie per accumulo energetico: tecnologie e rilievi sperimentali*" tesi di laurea triennale, 2013.

[18] I.Bono " *Studio comparativo tra impianti idroelettrici di pompaggio e batterie al litio in sistemi stand alone con generatori fotovoltaici*", Tesi di Laurea magistrale, 2017

[19] http://www.pveducation.org/pvcdrom/batteries.

[20] Ruud Kempener (IRENA), Paul Komor and Anderson Hoke (University of Colorado) - "*SMART GRIDS AND RENEWABLES - A Guide for Effective Deployment - IRENA International Renewable Energy Agency*",2013

[21] Smart Grids - Enel Distribuzione - http://www.fub.it/files/Green_ict.pdf - La Telegestione - Enel Distribuzione - Vantaggi - Enel Distribuzione, 2015

[22] I sistemi di accumulo elettrochimico: prospettive e opportunità – Anie Energia, 2017

[23] P. Kurzweil, "*Electrochemical Energy Storage for Renewable Sources and Grid Balancing", Chapter 16 "Lithium Battery Energy Storage: State of the Art Including Lithium–Air and Lithium–Sulfur Systems*", Pages 269-307, Elsevier, 2015.

[24] https://cleantechnica.com/2017/02/27/worlds-biggest-lithium-ion-energy-storage-facility

[25] Baljit Riar(Member IEEE), Jaehwa Lee, Alessandra Tosi, Stephen Duncan(Member IEEE), Michael Osborne, and David Howey(Member IEEE), "*Energy Management of a Microgrid: Compensating for the Difference between the Real and Predicted Output Power of Photovoltaics*",2016

[26] Nasim Jabalameli, Sara Deilami, Mohammad A.S. Masoum (Department of Electrical and Computer Engineering Curtin University, Perth, WA, Australia), Masoud Abshar (Magellan Power Bibra Lake WA, Australia), "*Rooftop PV with Battery Storage Solar Smoother*",2014